ARMY RESEARCH LABORATORY

Failure Analysis, Cadmium Brush Plate Qualification and Salt Fog Testing of the AH-64 Shock Strut Mount, P/N 7-311113409

by Marc Pepi

ARL-TR-2870

November 2002

20030115 139

NOTICES

Disclaimers

Army Research Laboratory

Aberdeen Proving Ground, MD 21005-5069

ARL-TR-2870   **November 2002**

Failure Analysis, Cadmium Brush Plate Qualification and Salt Fog Testing of the AH-64 Shock Strut Mount, P/N 7-311113409

Marc Pepi
Weapons and Materials Research Directorate, ARL

Abstract

A failure analysis was performed on a shock strut mount from an AH-64 Apache attack helicopter. It was concluded that the failure was attributed to stress corrosion cracking and/or corrosion fatigue and had initiated at a region where the protective cadmium plating was worn away in service. Based upon this conclusion, it was necessary to qualify two facilities (Hunter Army Air Field, Savannah, GA and Ft. Lewis, Dupont, WA) for the cadmium brush plating rework of these components found to have worn coatings during routine inspections. The U.S. Army Research Laboratory was involved in the qualification process for both facilities, and the results of each quality audit are included. Finally, the results of salt fog testing of cadmium brush plated specimens, plated at the respective facilities, are also included, as well as a comparison of the grain size of the material in the failed component vs. the material from the struts plated at each facility.

Contents

List of Figures

INTENTIONALLY LEFT BLANK.

List of Tables

INTENTIONALLY LEFT BLANK.

1. Introduction

The U.S. Army Research Laboratory (ARL) was tasked by the U.S. Army Aviation and Missile Command (AMCOM) to perform a failure investigation of an AH-64 Apache shock strut mount. This technical report summarizes the results of this analysis, as well as ARL's involvement in qualifying two Army facilities to cadmium brush plate worn strut mounts (Appendices A and B). Also included are the results of salt fog testing cadmium brush plated specimens from the two facilities (Appendix C), and grain size comparison of various specimens (Appendix D). Appendix E includes an AMCOM Deficiency Report based on the results of ARL's investigation, while Appendix F contains the updated Engineering Drawing, which included a material change and the addition of shot peening. The failure analysis report and appendices are entitled and dated as follows:

- Failure Analysis of an AH-64 Shock Strut Mount, Part 7-311113409 (Final version, 18 May 1998);

- Qualification of Hunter Army Air Field (HAAF), Savannah, GA for Cadmium Brush Plating Rework of Shock Strut Mounts (17 June 1997);

- Qualification of Ft. Lewis, Dupont, WA for Cadmium Brush Plating Rework of Shock Strut Mounts (8 April 1998);

- Salt Fog Testing of Cadmium Brush Plated Specimens from HAAF and Ft. Lewis (6 July 1998);

- Grain Size Comparison of Failed Strut Mount, HAAF Specimen and Ft. Lewis Specimen (26 October 1998);

- AMCOM Deficiency Report as a Result of ARL's Failure Investigation (22 January 1998);

- Change of Manufacturer's Engineering Drawing (undated).

2. Failure Analysis of an AH-64 Shock Strut Mount, Part 7-311113409

2.1 Background

AMCOM requested that ARL and the Weapons and Materials Research Directorate (WMRD) perform a failure analysis of an AH-64 shock strut mount, which is a component of the main landing gear assembly. The right hand (R/H) mount, which secures the R/H landing gear trailing arm to the fuselage failed in flight. It was the first of these mounts to fail during flight. Stress corrosion cracking (SCC), which initiates at the transition point between the base of the underside of the shaft and the mount base, has been attributed to numerous failures of this item in the past. This has been the result of cadmium wearing off and corroding away in service. The

part under investigation failed after 1148 flight hours, and the gross weight of the aircraft at the time of failure was 12,040 lb.

2.2 Manufacturing Criteria

Material: *18% Nickel Maraging Steel* per Hughes Material Specification (HMS) 6-1081, 300,000 psi grade.

Strength: *280,000 psi Ultimate Tensile Strength (UTS)* required per specification HMS 6-1081.

275,000 psi UTS required per MDHS drawing 7-311113409.

Treatment: Annealed at 1500 °F for 1 hr/in, cooled in air, then aged at 900 °F for 4–6 hr and cooled in air.

Coating: *Vacuum Cadmium Plating* (Finish 61A per EPB 4-230; MIL-C-8837, Class 2 equivalent [1]), followed by *Epoxy Primer* per MIL-P-23377, Type I, Class 3 [2].

2.3 Miscellaneous

Aircraft Flight Hours: 1148

Intended Service Life: Unlimited

2.4 Applicable Specifications

- McDonnell Douglas Engineering Drawing No. 7-311113409

- HMS 6-1081

- McDonnell Douglas Bulletin EPB 4-230

- McDonnell Douglas Process Specification HP 1-1

2.5 AH-64 Shock Strut Mount

The shock strut mount was fabricated in accordance with McDonnell Douglas Engineering Drawing No. 7-311113409-2. The component is part of the main landing gear and is located on the helicopter as shown in Figure 1. This figure also shows the location of the failure. The component is forged from Maraging 300 steel; and after heat treatment and final machining, it is cadmium coated using a vacuum deposition process. The part is subsequently painted using an epoxy primer. The failure of the part occurred at the radius separating the spindle from the base of the component. This region is subjected to the loads generated by the aircraft performing level and running landings. ARL examined a similar part, in which the failure occurred at the same location and was attributed to SCC and/or corrosion fatigue (CF) [3].

2
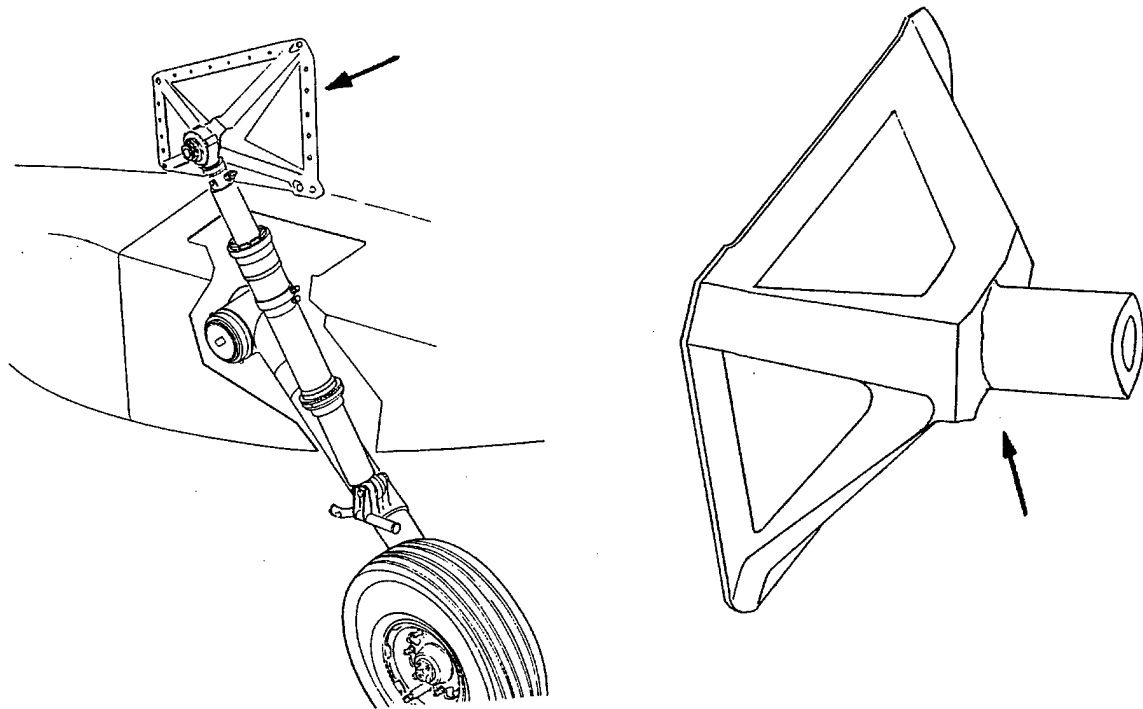
Figure 1. Schematic of the strut mount attached to the helicopter and the location of failure.

2.6 Visual Inspection/Light Optical Microscopy

Figure 2 shows the fracture surface of the sectioned component in the as-received condition. The part failed at the machined radius of the spindle section. Figure 3 is a close-up of the fracture surface using oblique lighting, showing the fracture features, such as shear lips and beach marks. Two distinct cracks were noted and labeled "primary" and "secondary," based upon the severity of corrosion on the fracture surface (the crack with the most severe corrosion was labeled primary, while the other was labeled secondary). These two crack fronts initially propagated on different planes and converged during fast fracture in the location shown in Figure 3. The size of the grains within these intergranular regions was so large that the resultant "rock candy" morphology was observed using light optical microscopy. Figures 4 and 5 show the intergranular morphology of the primary and secondary cracks, respectively. The green-colored primer was nonexistent along the length of the spindle, and the only evidence of the primer coating on the entire section was along the small portion of the shoulder shown in Figure 6. Visual evidence of the cadmium coating, as noted by white corrosion products, was only observed along the threads, as shown in Figure 7, and was not present anywhere else on the failed section. These coatings most likely wore off in service. The spindle itself showed areas of heavy corrosion and pitting. Figure 8 shows the radius adjacent to the primary origin. Note the corrosion pit that was only 0.031 in away from the fracture origin. Corrosion pits were also adjacent to the secondary origin, as shown in Figure 9. Corrosion pitting was prevalent along the spindle, and Figure 10 shows an example of a typical grouping of these pits within a corroded

3
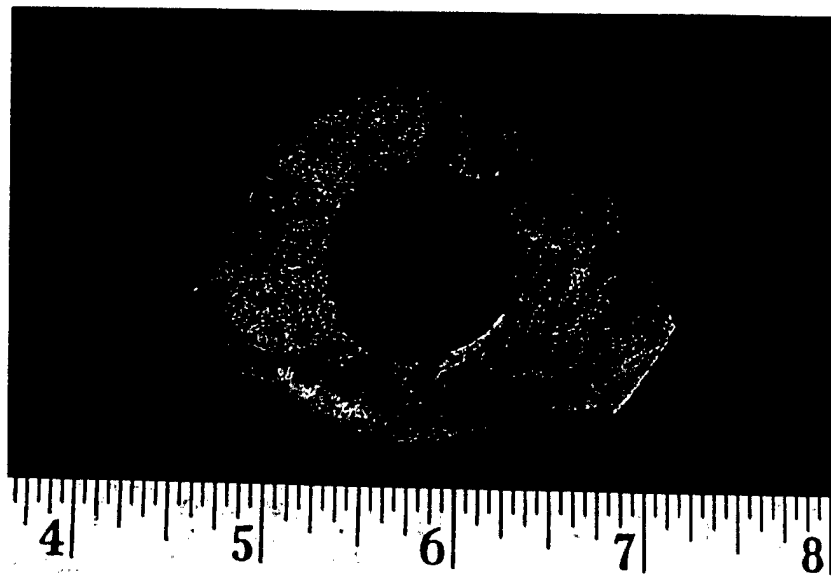
Figure 2. Fracture surface of the failed part in the as-received condition (mag. ~1×).

crack front convergence

beach marks

primary crack

shear lip   secondary crack
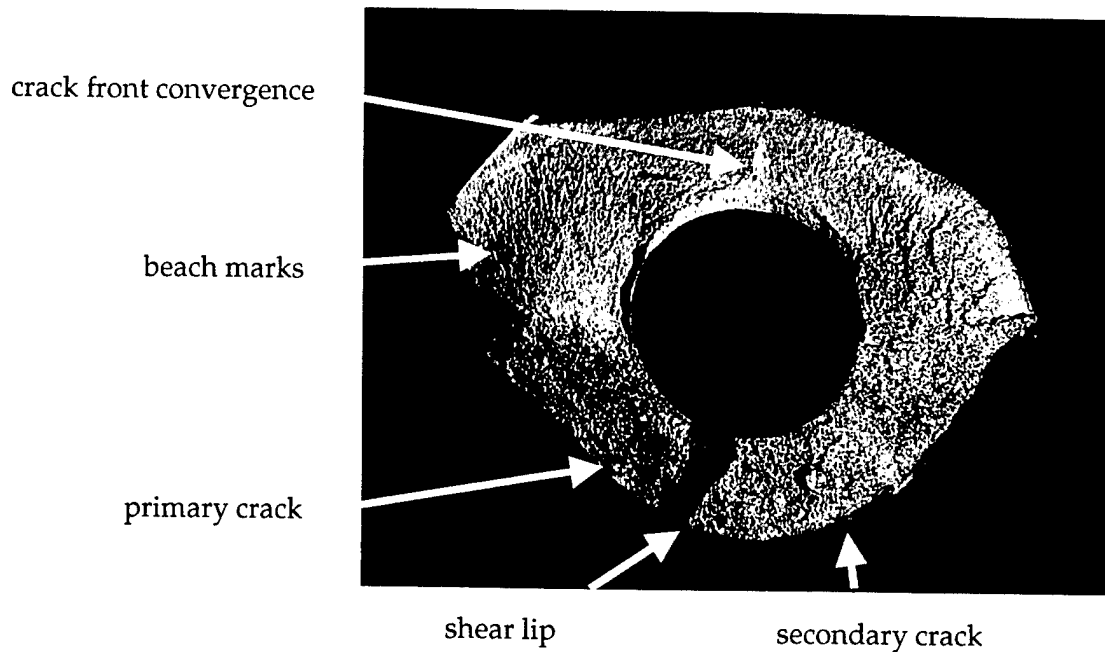
Figure 3. The fracture surface using oblique lighting. Note the shear lip separating the primary and secondary cracks, as well as the beach marks (mag. ~1.4×).

4
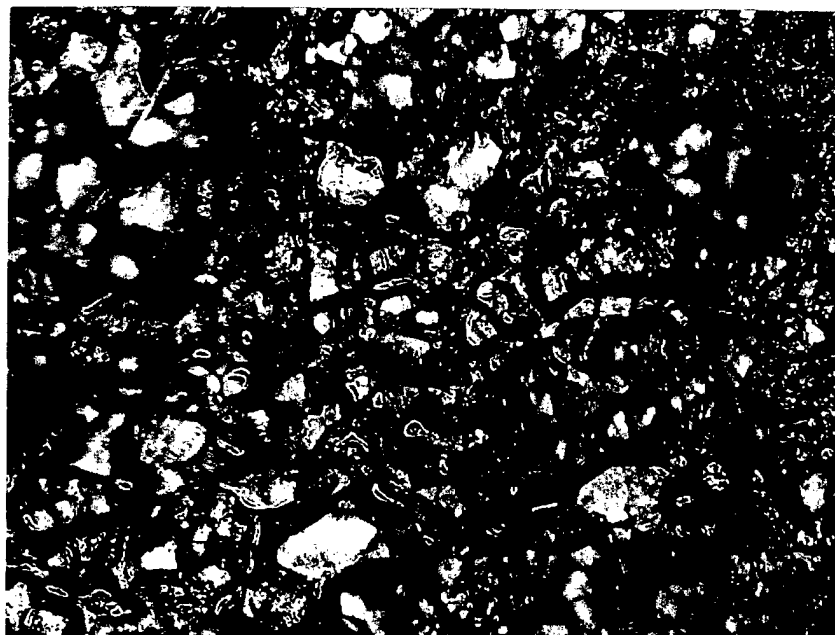
Figure 4. Intergranular morphology observed within primary crack using light optical microscopy (mag. 30×).
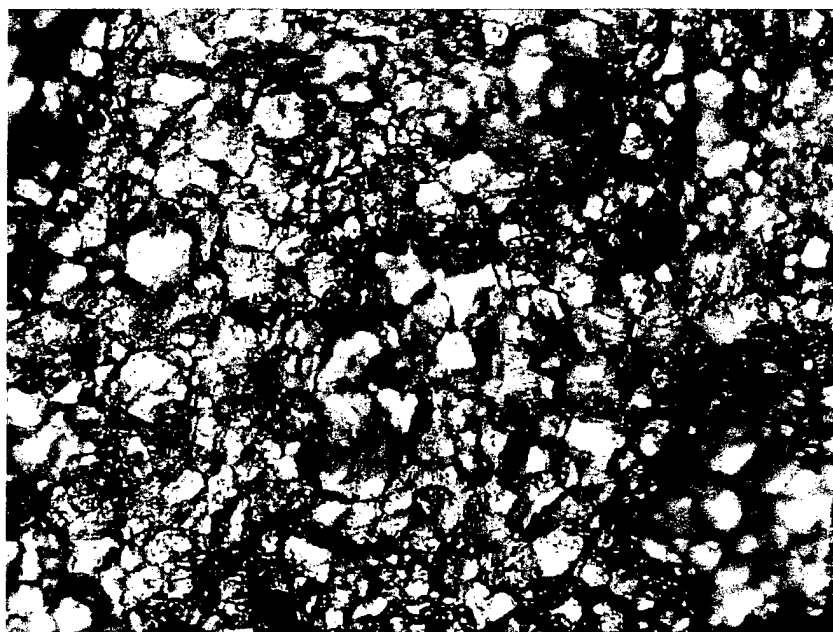
Figure 5. Intergranular morphology observed within secondary crack using light optical microscopy (mag. 30×).
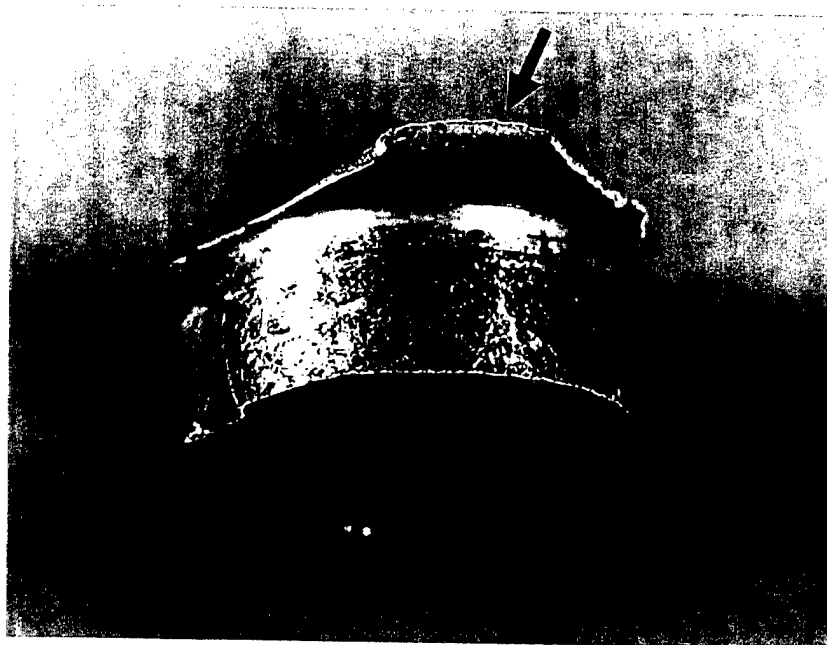
Figure 6. The only evidence of the green epoxy primer was along this small section of the shoulder.

Figure 7. The only evidence of cadmium on the failed part was in the threads, shown here as a white, powdery corrosion product energy dispersive spectroscopy (energy dispersive spectroscopy [EDS] confirmed the presence of cadmium) (mag. ~1.5×).

fracture surface

corrosion pit

Fracture origin
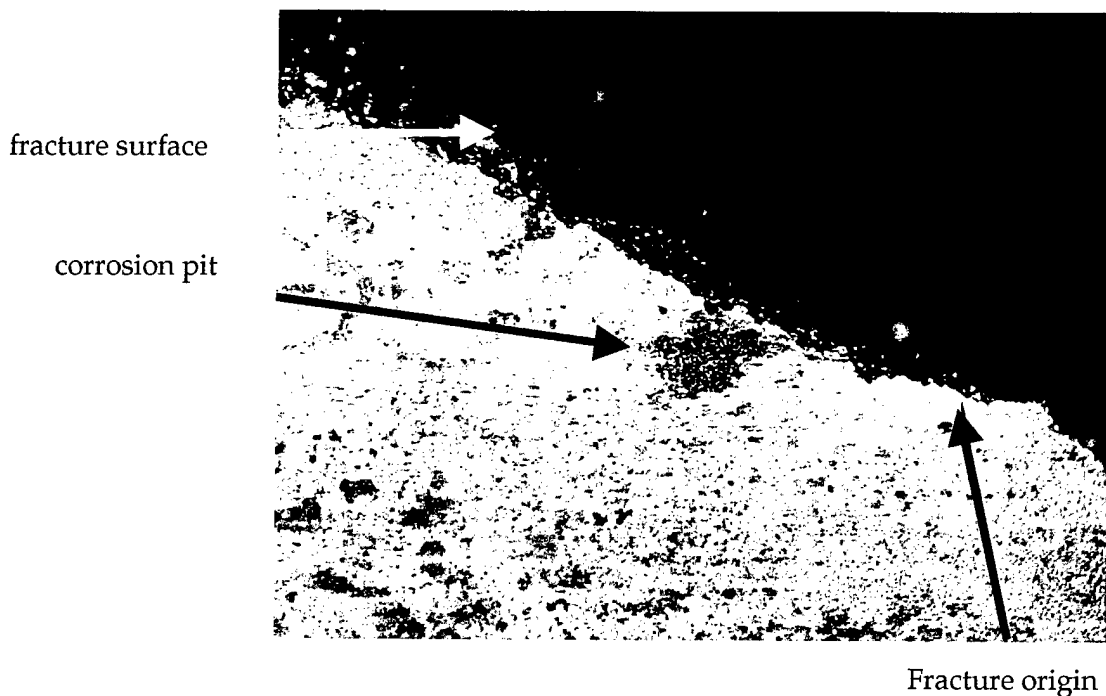
Figure 8. Corrosion pits adjacent to the primary origin (mag. 10×).

fracture surface

fracture origin

corrosion pits

Figure 9. Corrosion pits adjacent to the secondary origin (mag. 10×).

region. Also observed was a competing crack that was adjacent to the primary origin. Figure 11 shows the intergranular nature of this crack. There was also evidence of intergranular attack along this crack path. It was difficult to discern the exact location of the fracture origins; however, based upon the heavy corrosion in certain areas on both the primary and secondary crack surfaces, the general location of the origins was surmised.

Figure 10. Group of pits observed along the spindle of the failed part. Pitting was prevalent along the spindle region (mag. 25×).

Intergranular attack

Figure 11. Competing crack path adjacent to primary fracture surface. Note the intergranular nature of the crack, as well as the region of intergranular attack (mag. 15×).

2.7 Metallography

A section of material was taken approximately 3/4 in away from the fracture plane, such that metallographic examination could be performed. A transverse and longitudinal sample were polished then etched with Marble's reagent (4-g $CuSO_4$, 20-mL HCl, and 20-mL deionized water). The structure was similar in both orientations and is shown in Figures 12 and 13. The structure was typical of Maraging 300 steel, consisting of an aged, low-carbon martensite. In addition, the material was fairly clean, exhibiting no gross defects or inclusions and containing no appreciable decarburization. However, the structure was not consistent with the prior treatment (annealed at 1500 °F for 1 hr/in, cooled in air, then aged at 900 °F for 4–6 hr and cooled in air). Section 3.4.1.3 of specification HMS 6-1081 requires a grain size of no. 7 or finer with an occasional no. 5 unless otherwise specified for material up to 3 inches in diameter or square. The grain size was determined using four different methods: (1) American Society for Testing and Materials (ASTM) E112 [4] charts overlaid onto photomicrographs at 100×, (2) using a metallograph with grain size reticle, (3) by means of an incremented ruler reticle, and (4) examining SEM micrographs of the intergranular fracture. The grain size of this material was

Figure 12. Microstructure of the material showing aged, low-carbon martensite in the longitudinal direction. Marble's Reagent (mag. 50×).

9

Figure 13. Microstructure similar to that in Figure 12 shown at higher magnification and in the transverse direction. Marble's Reagent (mag. 100×).

between nos. 2 and 3 at 100× magnification using the ASTM E112 charts over Figure 12. To verify this, a photomicrograph was taken using a grain size reticle, as shown in Figure 14. Again, the size was between nos. 2 and 3. The ASTM E112 charts indicate that the nominal diameter of the average grain is between 0.005 and 0.007 in, respectively for a grain size of nos. 3 and 2. A photomicrograph was subsequently taken of this structure at 100×, using an incremented reticle (Figure 15). As shown, the grain appear to have diameters ranging from 0.005–0.01 in, which correlated to the previous measurements. Subsequently, the intergranular fracture surface shown in Figure 18 (also see section 2.8) was also examined for grain size using the ASTM E112 "Fracture Grain Size" method. This technique is typically used for high-hardness, brittle steels with a predominantly martensitic structure, such as tool steels, high-carbon steels and martensitic stainless steels, and should be done with the specimen in the as-quenched or lightly tempered condition. Even though the Maraging 300 steel is a low-carbon alloy, the results obtained compared favorably to those from the other three methods. From Figure 18, the grain size ranged from ~100–200 μm, which correlated to a range of 0.004–0.008 in.

2.8 Electron Microscopy/EDS

The fracture surface of the component was subsequently examined using the scanning electron microscope (SEM) in order to determine the fracture morphology and fracture mechanism. The fracture surface was ~50% intergranular (the primary crack comprised 20%, while the secondary crack was 30%). Figure 16 is a schematic showing the fractographic features of the surface. The

10

Figure 14. Microstructure of the material with grain size reticle overlay. The grain measured between nos. 2 and 3. Marble's Reagent (mag. 100×).

Figure 15. Microstructure of the material with incremented reticle overlay. The grain size measured between 0.005 and 0.01 in. Marble's Reagent (mag. 100×).

crack front convergence

secondary crack plane (transgranular/ductile)

24

primary crack plane
(transgranular/ductile)

23

22

secondary origin

primary crack (intergranular)

17 19

secondary crack (intergranular)

18

primary origin   shear lip   20 21
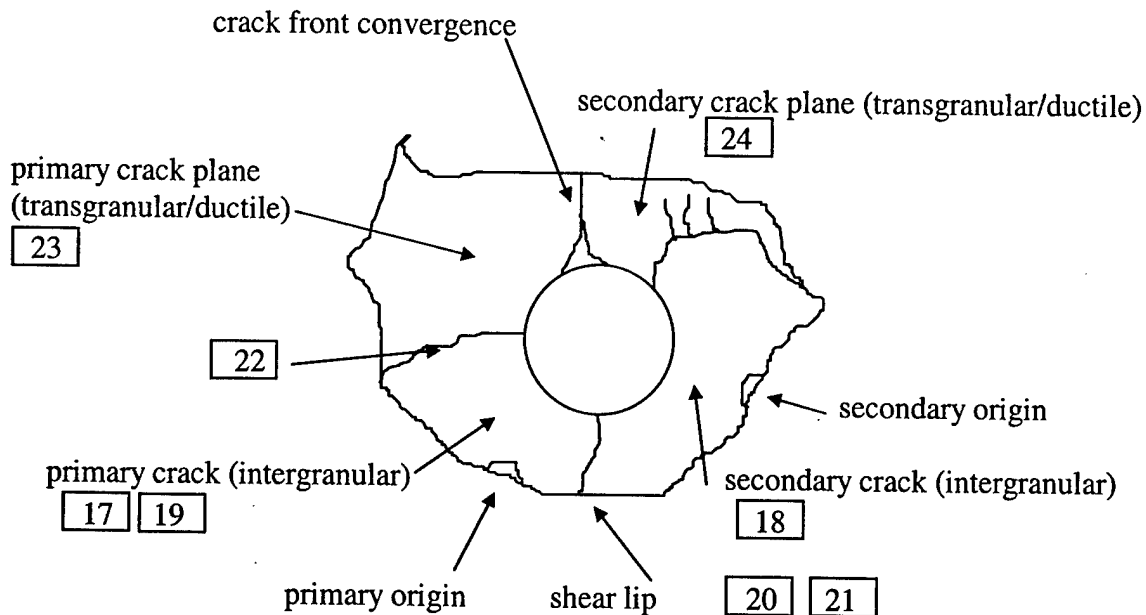
Figure 16. Schematic of fracture features as determined through SEM. Numbers in boxes correspond
to figure locations.

morphology of the both the primary crack and the secondary crack was intergranular, as shown
in Figures 17 and 18. Note the textbook "rock candy" morphology and the secondary cracking
typical of a brittle fracture. Figure 19 (taken within the secondary crack fracture surface) shows
this morphology at increased magnification. Note the evidence of micro-pores, which are typical
of 18% nickel maraging steel hydrogen-assisted failures [5]. These two crack fronts were
separated by a shear lip, which failed in a ductile manner, as evidenced by the morphology
shown in Figure 20. Figure 21 shows the transition zone between the secondary crack and the
adjacent shear lip that separated the two crack fronts. Figure 22 shows the transition zone
between the primary crack and the transgranular/overload morphology. This was also typical of
the transition zone between the secondary crack and the transgranular/overload region.
Figures 23 and 24 show the transgranular/overload morphology that made up ~45% of the
fracture surface. Figure 25 shows this morphology at higher magnification. As shown, this
surface morphology represents very low cycle fatigue, in which the loading produces not only
the transgranular morphology typical of fatigue, but also ductile dimples indicative of tensile
overload. No fatigue striations were discernible within the transgranular/overload regions. An
attempt was made to examine the fracture origins; however, the corrosion, as well as the nature
of brittle failures, made it difficult to pinpoint the exact sites with 100% accuracy.
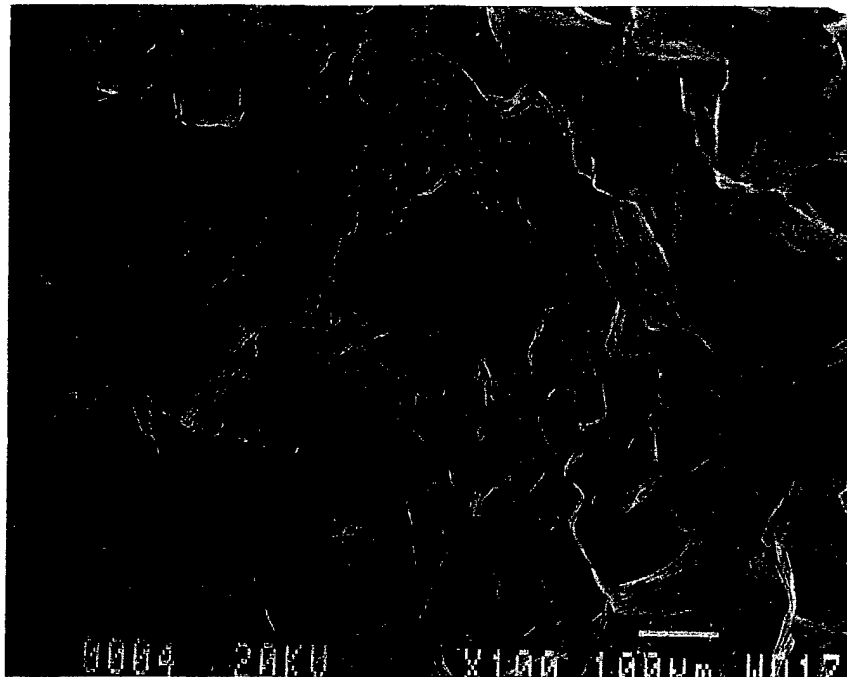
Figure 17. Morphology of the primary fracture surface. "Rock candy" was prevalent within this region (mag. 100×).
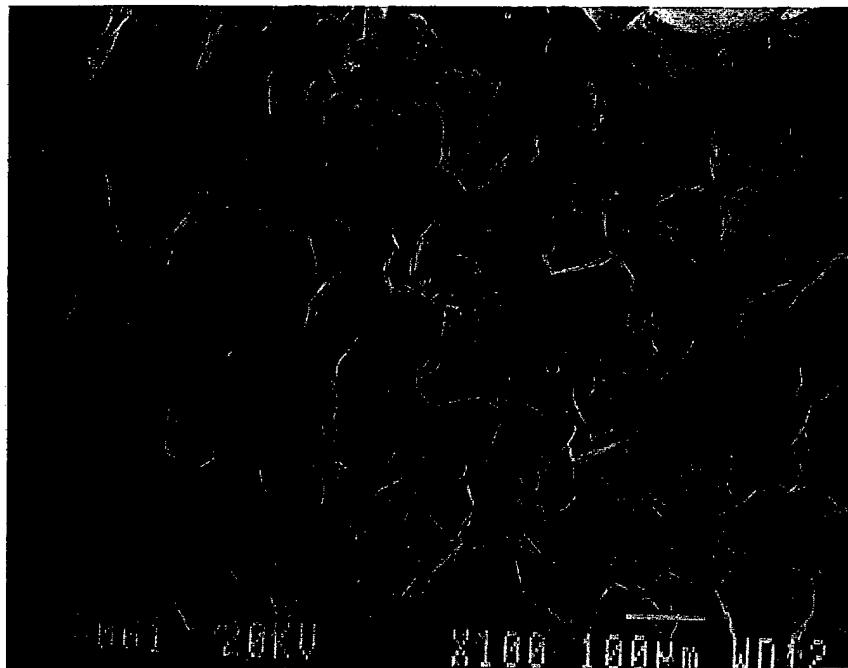
Figure 18. Morphology of the secondary fracture surface. "Rock candy" was prevalent within this region (mag. 100×).

13

Figure 19. Magnified view of the intergranular morphology showing secondary cracking (mag. 200×).
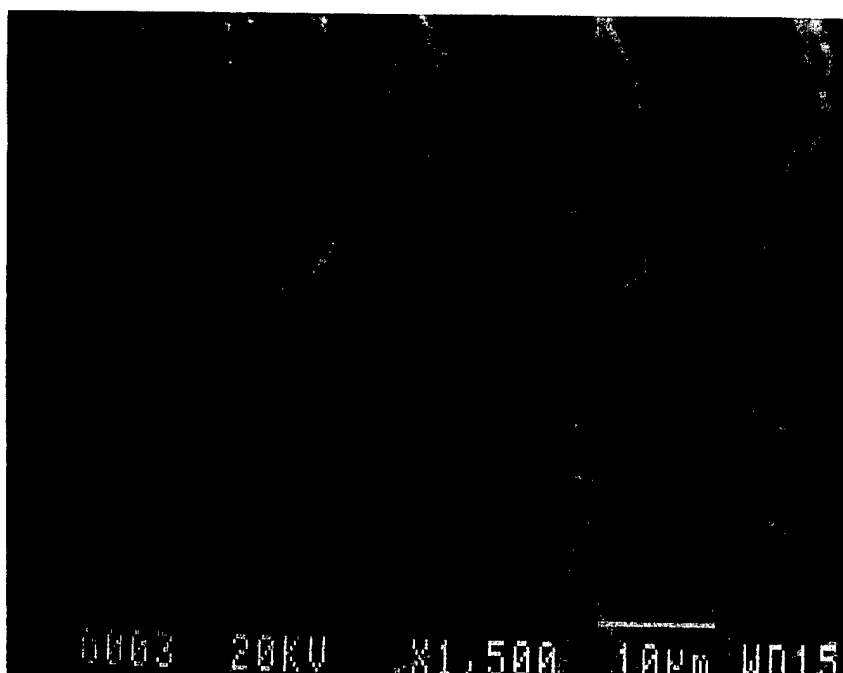
Figure 20. Ductile morphology noted within shear lip between the primary and secondary fracture (mag. 1500×).

14
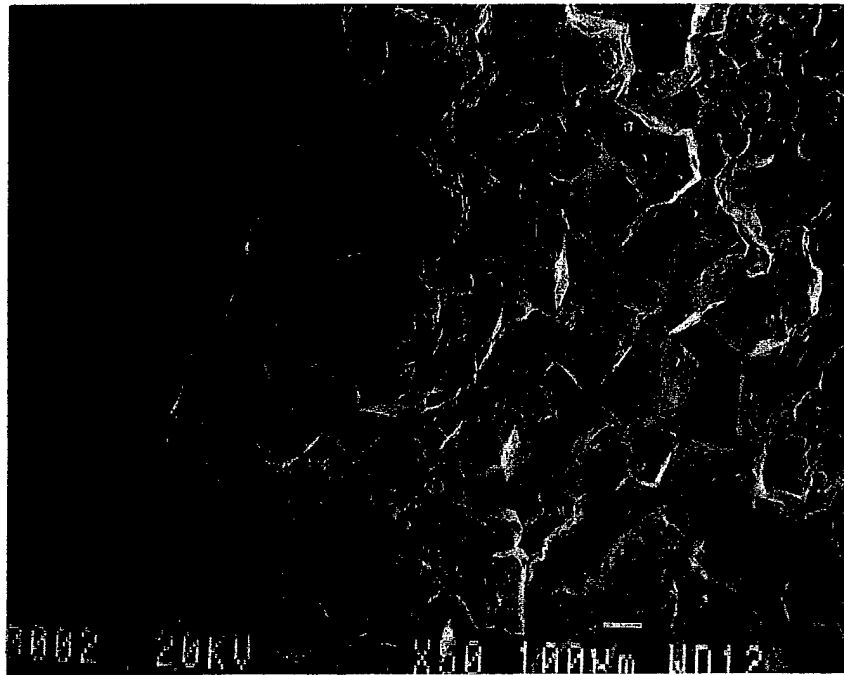
Figure 21. Interface between the secondary fracture surface and the shear lip (mag. 50×).
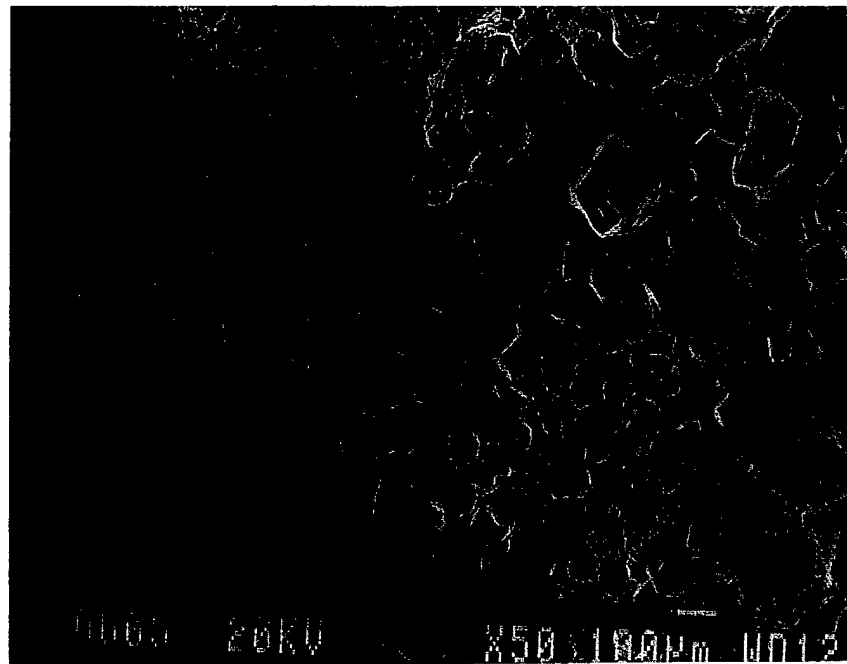
Figure 22. Interface between the primary fracture surface and the transgranular/ overload region (mag. 50×).

15
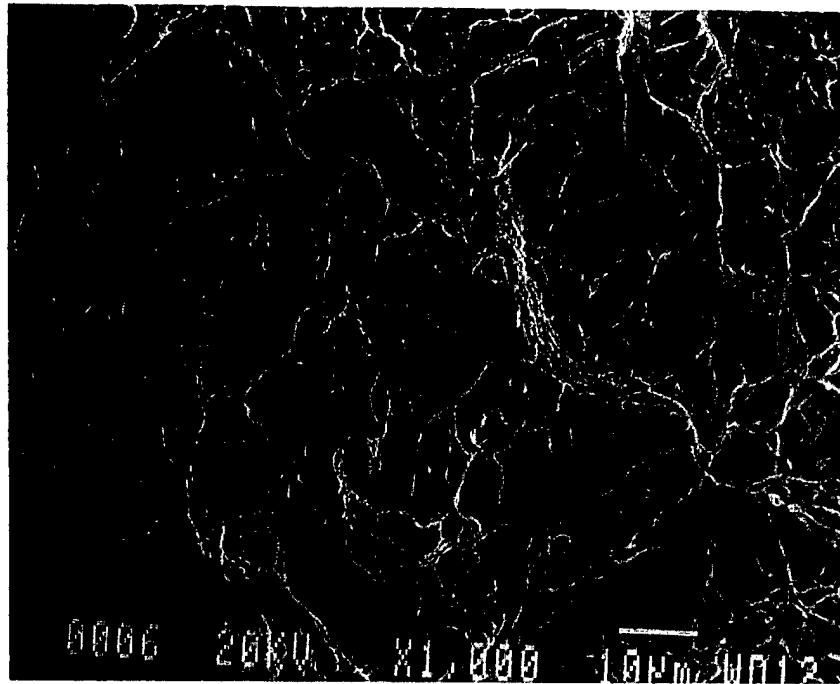
Figure 23. Morphology of the surface on the same plane as the primary fracture
surface subjected to fast-fracture, consisting of a transgranular/
ductile mode (mag. 1000×).
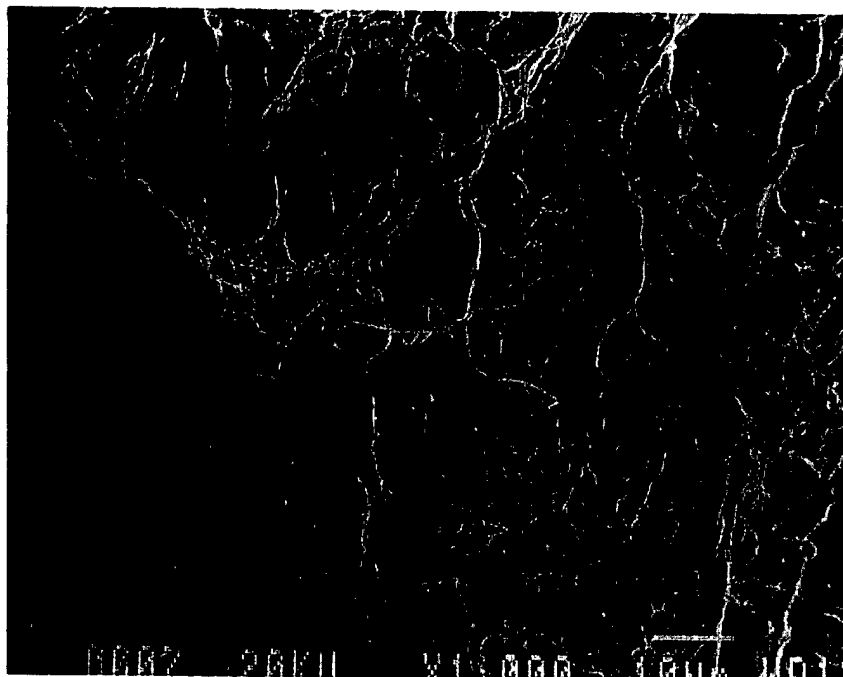
Figure 24. Morphology of the surface on the same plane as the secondary
fracture surface subjected to fast-fracture, consisting of a
transgranular/ductile mode (mag. 1000×).

16
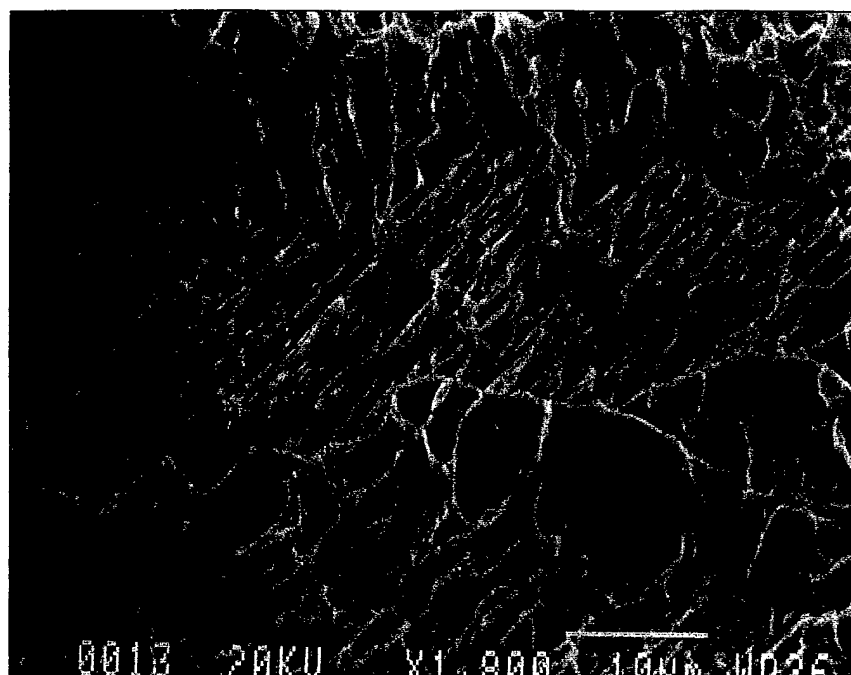
Figure 25. Transgranular/ductile morphology at higher magnification
(mag. 1800×).

EDS was used in an effort to determine the presence of cadmium on the surface of the spindle. Exhaustive EDS spectra were generated along the spindle (and adjacent to the fracture origins), without revealing the presence of cadmium. Figure 26 is typical of the spectra generated in these regions. In contrast, analysis of the threaded region (where white, powdery corrosion products were noted) revealed the presence of cadmium as shown in Figure 27. The wear within the threads may not have been as severe as along the spindle, such that the cadmium was still somewhat intact. This was evidence that the part had been cadmium coated at one time.

Paragraph 3.3.3d of Process Specification HP 1-1, "Steel, Nickel-Base and Cobalt-Base Alloys, Heat Treatment of," states that maraging steel bars and forgings shall exhibit an aged martensitic structure, fine grained, with no evidence of titanium-carbonitride at the grain boundaries. The mounted samples were repolished and etched with ferric chloride (5-g $FeCl_3$, 50-mL HCl, and 50 mL of distilled water) in order to reveal the austenitic grain boundaries. EDS was subsequently used to determine the chemical composition of precipitates noted within the grain boundaries. Figure 28 shows an example of one of these precipitates (see white arrow). EDS of this precipitate (Figure 29) revealed a small amount of titanium, but no carbon or nitrogen. EDS was subsequently conducted on the intergranular fracture surface, in an attempt to locate Ti (C, N) precipitates along the grain boundaries. Figure 30 shows a precipitate on a grain boundary of the "rock candy" surface that was analyzed. The resultant spectrum is displayed in Figure 31. Note the high level of titanium as well as the presence of carbon and nitrogen. This was evidence of a titanium-carbonitride at the grain boundaries. Figure 32 shows an additional precipitate that revealed a similar spectrum.

17
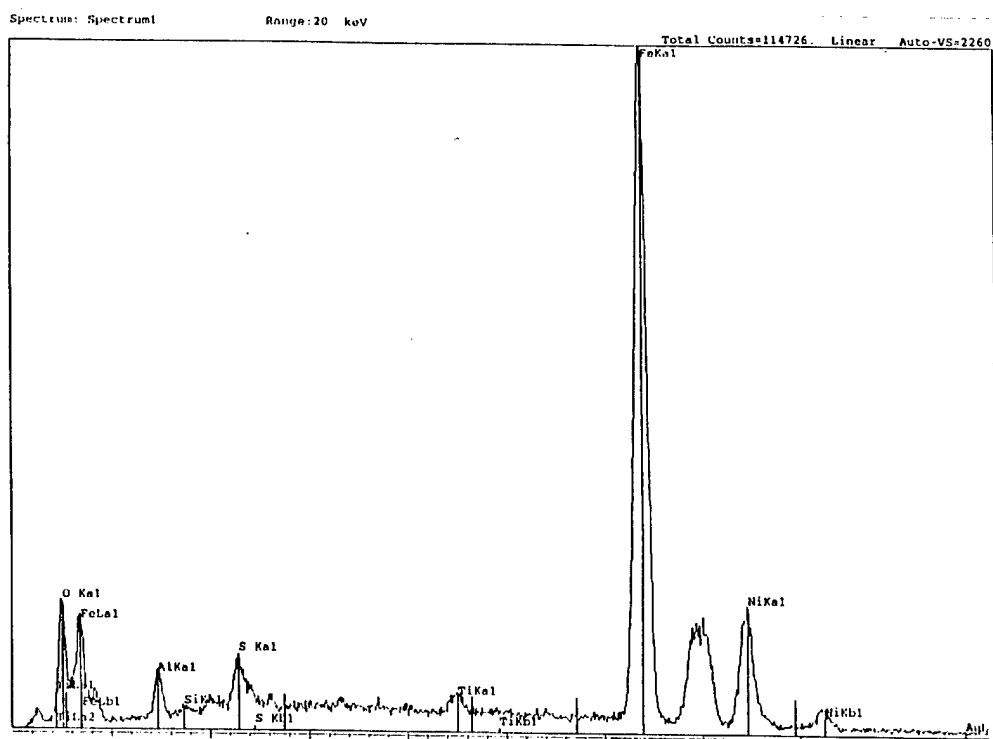
Figure 26. Representative EDS spectra of the spindle of the failed part. No evidence of cadmium
          was noted along the spindle.
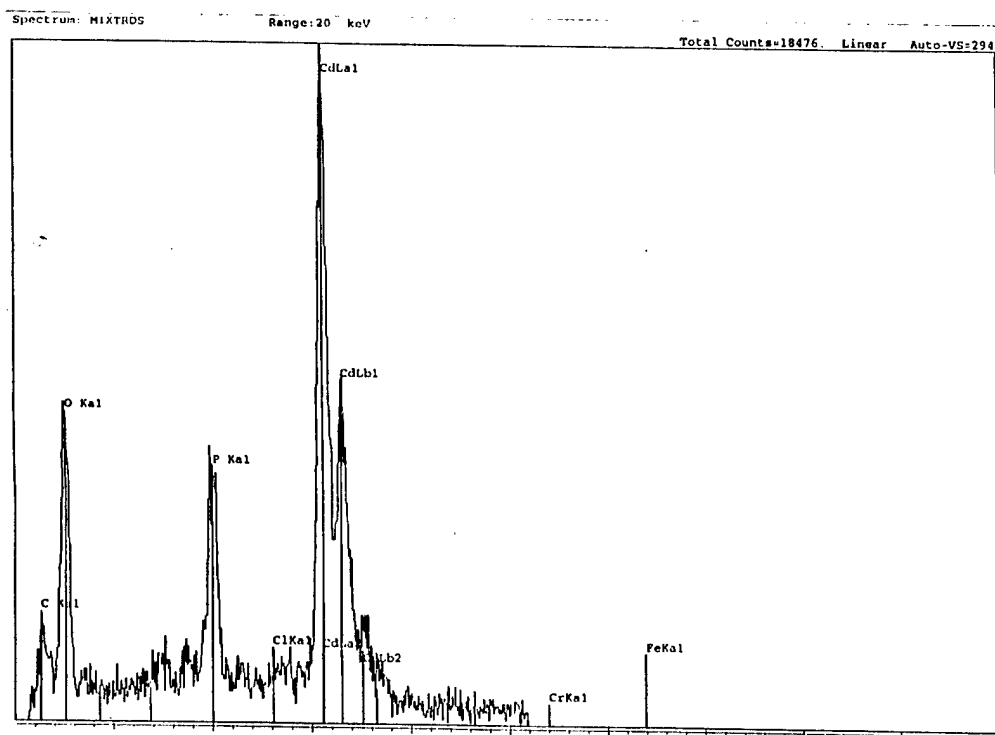
Figure 27. Representative EDS spectra within the threads of the failed part. Cadmium was noted
          within the threads.

Gr boundaries
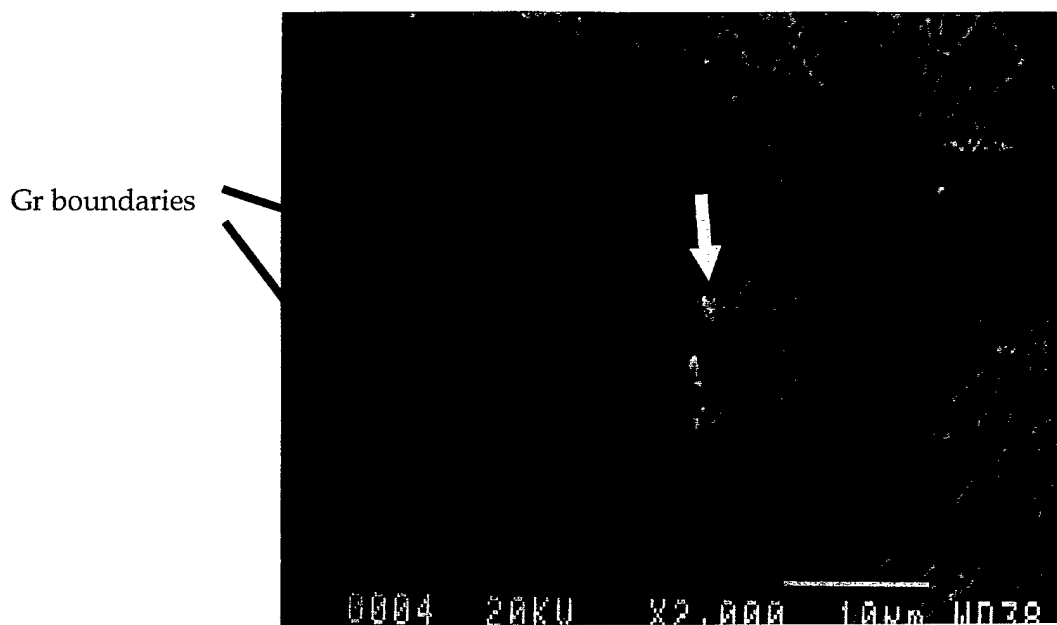
Figure 28. SEM micrograph of polished and etched surface showing titanium precipitate (white arrow) within a grain boundary that was subjected to EDS (mag. 2000×).
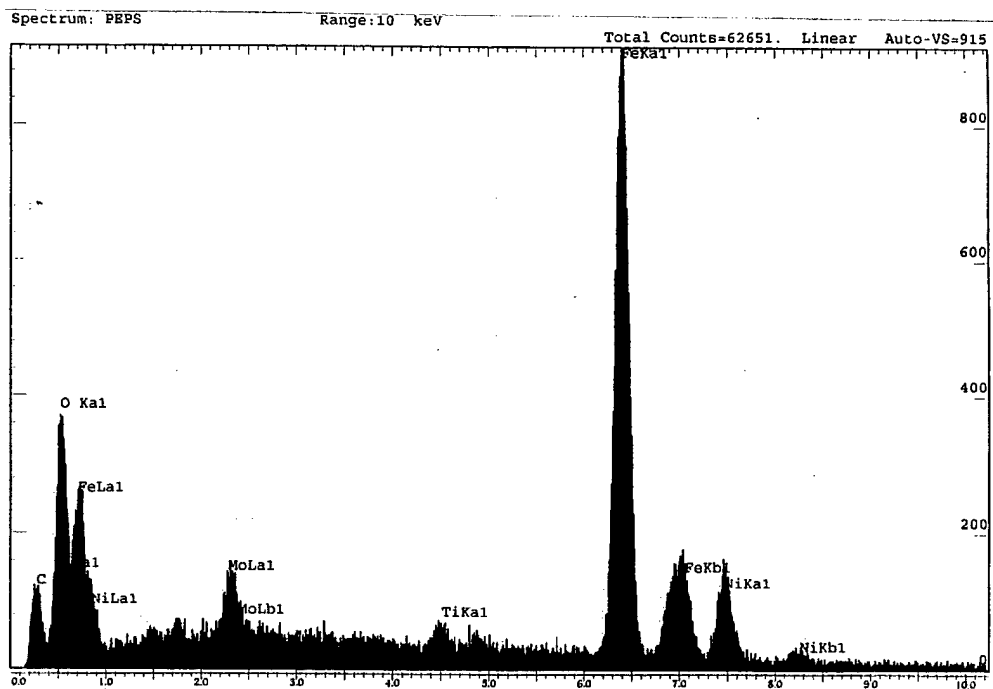
Figure 29. EDS spectra showing evidence of titanium within the precipitate shown in Figure 28. Other elements constitute the alloy.
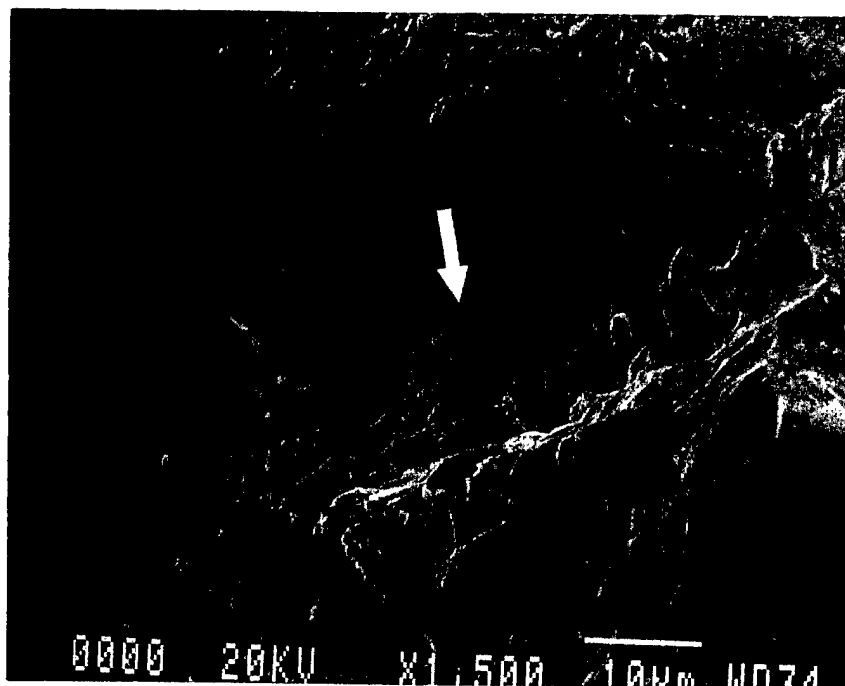
Figure 30. SEM micrograph of intergranular morphology of the primary
fracture, showing the titanium-carbonitride precipitate that was
examined using EDS (Figure 31) (mag. 1500×).
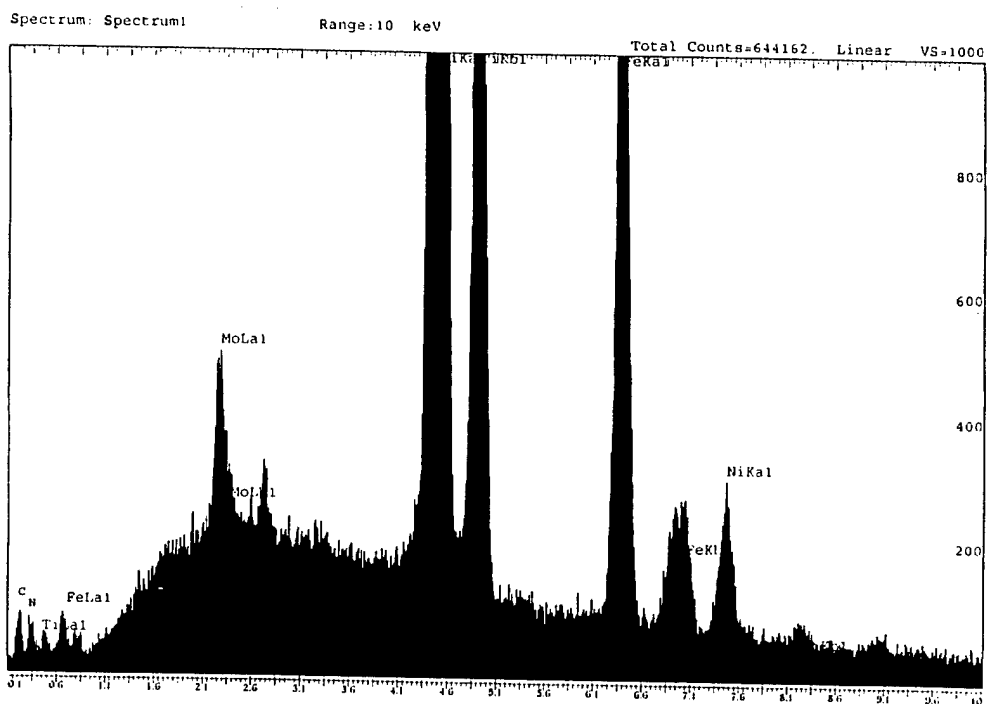
Figure 31. EDS spectra of the Ti (C, N) precipitate shown in Figure 30. Note the presence of
titanium, carbon, and nitrogen, as well as the alloying elements.

20
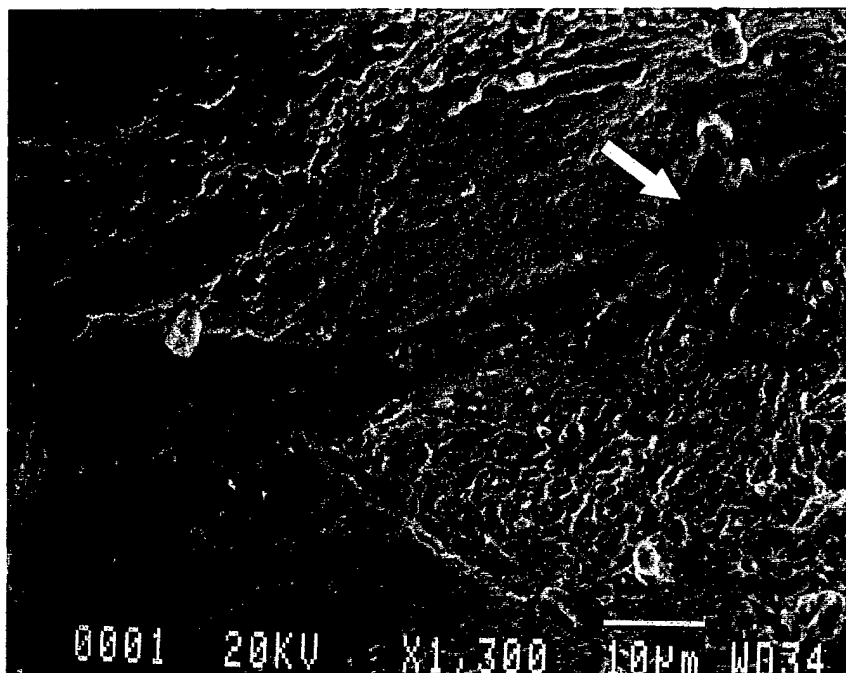
Figure 32. SEM micrograph of intergranular morphology of the primary
fracture, showing another titanium-carbonitride precipitate
(mag. 1300×).

2.9   Chemical Analysis

A section of the shock strut mount was analyzed in order to determine the chemical composition
of the alloy. The material was required to conform to Specification HMS 6-1081. The
composition was determined by the Leco combustion method (carbon and sulfur) and inductively
coupled argon plasma emission spectroscopy. The material met the requirements of
HMS 6-1081, as listed in Table 1.

2.10 Hardness Testing

Rockwell hardness testing was conducted on the failed component, as well as the mounted
samples used for metallography. The part is required to exhibit a hardness between HRC 50–54,
in accordance with HMS 6-1081. The average of six readings taken along the cylindrical spindle
conformed to this requirement, as shown in Table 2.

Table 3 contains the results of hardness testing on the mounted metallographic samples,
representing the longitudinal and transverse orientations of the component.   A total of five
readings were taken on each sample. The results conformed to the governing requirement.

21

Table 1. Chemical composition (weight-percent).

Element	Failed Component	HMS 6-1081
Carbon	0.012	0.03 max.
Nickel	18.5	18.0–19.0
Cobalt	9.12	8.5–9.5
Molybdenum	4.88	4.6–5.2
Titanium	0.65	0.50–0.80
Aluminum	0.12	0.05–0.15
Copper	0.23	0.25 max.
Tungsten	0.036	0.25 max.
Chromium	0.22	0.25 max.
Manganese	0.042	0.10 max.
Silicon	0.081	0.10 max.
Phosphorus	0.001	0.010 max.
Sulfur	0.003	0.010 max.
Zirconium	0.012	0.020 max.
Boron	0.0026	0.003 max.
Calcium	0.0014	0.050 max.
Iron	remainder	remainder

Table 2. Hardness readings on spindle
Rockwell "C" scale.

Reading	HRC
1	52.5
2	50.9
3	52.0
4	49.8
5	51.3
6	52.9
Average	51.6
HMS 6-1081	50–54

2.11 Discussion

2.11.1 Maraging 300 Grain Size

The grain size of this material was determined to be approximately twice as large as required. The nominal grain size of no. 7 or finer as specified in HMS 6-1081 is to be expected from annealing this material at the 1500 °F requirement and can be expected after annealing up to a temperature of ~1800 °F, while a grain size of no. 4 can be expected after annealing at 2100 °F, and as large as no. 0 after annealing at 2300 °F [6]. It has also been stated that a grain size of no. 1.5 could be expected at 2100 °F, no. 4 at 1880 °F, and no. 7 after three more cycles at 1880 °F [7]. Figure 2 of reference [8] shows the course grain (size no. 2) of 18% Nickel maraging steel that had been annealed at 2200 °F. Further, the *ASM Source Book on Maraging Steels* [9] states that grain size remains at no. 7 until the annealing temperature between 1700 °F and 1900 °F was

Table 3. Hardness readings on metallographic samples Rockwell "C" Scale.

Reading	HRC
Transverse	
1	51.4
2	51.7
3	51.4
4	51.6
5	51.2
Average	51.5
Longitudinal	
1	50.5
2	51.3
3	51.9
4	51.6
5	52.7
Average	51.6
HMS 6-1081	50–54

reached, and that annealing above 1900 °F increased the grain size rapidly to no. 1 at 2100 °F. The general trend is that the grain size increases with increasing annealing temperatures.

2.11.2 Effect of Grain Size on Mechanical Properties

It is well documented that increased grain size leads to a reduction in the tensile and fatigue properties. However, the UTS of Maraging 300 steel drops only slightly (~10 ksi), as a result of annealing temperatures from 1600 °F to 1900 °F [10]. As mentioned earlier, these temperatures correspond to grain sizes of approximately no. 7 to no. 4. This is consistent with the fact that the hardness of the part under investigation still met the governing requirement. However, fatigue life decreases progressively as annealing temperatures are raised above 1400°–2200 °F, and fatigue life shows little to no correlation with UTS for this alloy [8]. As the solution annealing temperature is raised, the fatigue fractures became increasingly intergranular in nature. It has been shown that a large austenite grain size is beneficial to toughness when direct rapid quenches from the annealing range is employed [8]. However, this condition is detrimental upon air cooling (as required for this alloy) or intermediate holding [11].

2.11.3 Effect of Grain Size on Resistance to SCC

Stavros and Paxton [12] is a study of the SCC behavior of Maraging 300 steel. The material was subjected to different annealing temperatures ranging from 1400 °F to 1830 °F (grain size nos. 9–4). It was concluded that cracking in fine-grained material that was produced by lower annealing temperatures branched extensively thus increasing the time to failure relative to the nonbranching case. It is highly likely that the large grain noted within the part under investigation contributed to the SCC failure.

2.11.4 Vacuum-Deposited Cadmium Coating

The part is required to be cadmium coated using the vacuum deposition method, per Finish 61A per EPB 4-230 (MIL-C-8837, Class 2 equivalent). The coating thickness is required to be 0.00030-in minimum. ARL attempted to determine whether the coating was indeed vacuum deposited, rather than electrodeposited. However, there was not sufficient coating remaining on the part to perform this task. An improperly applied, or non-post-baked electrodeposited coating could have imparted nascent hydrogen into the component, which is potentially detrimental. The vacuum process does not contaminate the subject part with hydrogen, and therefore, would not be considered contributory to this type of failure if applied in accordance with the governing specification.

2.11.5 Hydrogen-Assisted Failures

Maraging 300 steel, because of its high strength, can fracture under low stress when exposed to hydrogen in a corrosive environment. Nascent (or atomic) hydrogen is formed by the corrosion process (evident on the fracture surface of the part under investigation) and can migrate into the material causing failure by embrittlement. This hydrogen permeates into the areas of high-stress concentration, such as pits, defects, inclusions, voids or crack tips. The hydrogen required to cause embrittlement decreases as the strength of the material increases. Hydrogen can induce SCC, and hydrogen-assisted fractures in Maraging 300 steel occurs by intergranular decohesion, as exhibited in the material under investigation.

2.11.6 SCC and CF

SCC occurs in service only if all three of the following conditions are met: (1) the alloy has to be susceptible to SCC, (2) there must be a corrosive environment, and (3) a tensile stress is present in the form of actual loading or residual stresses. The morphology of SCC fractures are usually intergranular (hydrogen-assisted), but can be transgranular due to anodic dissolution. CF occurs when a part is subjected to a corrosive environment that reduces the fatigue resistance. CF failures are difficult to distinguish from SCC failures because both exhibit intergranular and transgranular morphologies [3]. The fracture surface of the strut mount exhibited beach marks that were the result of pauses in crack propagation. Beach marks are usually associated with cyclic loading (fatigue), but may also be formed during SCC by differences in the rate or degree of corrosion and/or crack growth on different planes.

2.11.7 Titanium-Carbonitrides

The presence of titanium-carbonitrides [Ti (C, N)] within the austenitic grain boundaries of this alloy is prohibited per Specification HP 1-1. This is due to the fact that these intermetallic precipitates, formed during cooling or intermediate isothermal holding below 2000 °F (usually 1500°–1800 °F), have been shown to drastically reduce toughness in this alloy [11]. Evidence of these precipitates at the grain boundaries suggested that a higher than optimal annealing temperature was most likely used by the contractor.

2.12 Failure Scenario

The failure of the shock strut mount occurred after the protective vacuum-deposited cadmium coating was worn off and corroded away at the radius in service. Corrosion pits developed along the radii that were prime crack origination sites. The corrosion process allowed nascent (atomic) hydrogen to migrate into the high-strength component causing SCC and/or CF. The part had a larger than acceptable grain size, and unacceptable titanium-carbonitride precipitates were detected along the grain boundaries, which offered decreased resistance to SCC.

2.13 Conclusions

- The cadmium coating along the spindle and radius was worn off and corroded in service.

- Pitting corrosion occurred along the radius and spindle, leading to a hydrogen-assisted failure resulting from SCC and/or CF.

- The grain size was approximately double the required size, most likely caused from a higher than nominal annealing temperature. The large grains offered less resistance to fatigue and SCC.

- Titanium-carbonitrides were detected on the grain boundaries of this material. This phase is formed at higher annealing temperatures (as is larger grain size) and tends to embrittle the alloy. The phase may have contributed to the intergranular SCC attack.

2.14 Recommendations

- Cadmium Plating: Numerous shock strut mounts have failed in the same location. A common link to each failure is the fact that the cadmium coating along the spindle and radius is worn off and corroded away, leading to corrosive attack. The use of a dry film lubricant could reduce wear in these regions.

- SCC and CF: A stress analysis or instrumented field test could be performed on the part to determine the magnitude of loading during worst case scenarios (hard landing, etc.). If loading is well below the threshold for Maraging 300, a material with less notch sensitivity and greater corrosion may be suitable, such as 200–250 Maraging steel.

- Heat Treatment: The manufacturer should exercise greater care and workmanship during the heat treatment of this alloy. Higher than nominal annealing temperatures have been shown to produce larger grain in this alloy, as well as detrimental titanium-carbonitride precipitates. These features decrease resistance to SCC and CF.

INTENTIONALLY LEFT BLANK.

3. References

1. U.S. Department of Defense. *Plating, Cadmium, Vacuum Deposited.* MIL-C-8837, Washington, DC, 2002.

2. U.S. Department of Defense. *Epoxy-Polymide Primer.* MIL-P-23377, Washington, DC, 2002.

3. Champagne, V. K., and G. Wechsler. "Failure Analysis of the Shock Strut Mount Located on the AH-64 Apache Helicopter." Letter Report, U.S. Army Ballistic Research Laboratory, Aberdeen Proving Ground, MD, 10 May 1991.

4. American Society for Testing and Materials. "Standard Test Methods for Determining Average Grain Size." ASTM E112, West Conshohocken, PA, 1996.

5. Engel, L., and H. Klingele. *An Atlas of Metal Damage.* Englewood Cliffs, NJ: Prentice-Hall Inc., p. 130, 1981.

6. Floreen, S., and R. F. Decker. "Heat Treatment of 18% Ni Maraging Steel." *ASM Source Book on Maraging Steels*, p. 23, 1979.

7. Saul, G., J. A. Roberson, and A. M. Adair. "The Effects of Thermal Treatment on the Austenitic Grain Size and Mechanical Properties of 18% Ni Maraging Steels." *ASM Source Book on Maraging Steels*, p. 55 (Figure 4), 1979.

8. Birkle, A. J., D. S. Dabkowski, J. P. Paulina, and L. F. Porter. "A Metallographic Investigation of the Factors Affecting the Notch Toughness of Maraging Steels." *ASM Source Book on Maraging Steels*, p. 127 (Figure 2), and p. 130, 1979.

9. Tuffnell, G. W., D. L. Pasquine, and J. H. Olson. "An Investigation of the Fatigue Behavior of 18% Nickel Maraging Steel." *ASM Source Book on Maraging Steels*, p. 77, 1979.

10. Carter, C. S. "Fracture Toughness and Stress Corrosion Cracking Characteristics of a High Strength Maraging Steel." *ASM Source Book on Maraging Steels*, p. 181 (Figure 1), 1979.

11. Kalish, D., and H. J. Rack. "Thermal Embrittlement of 18% Ni Maraging Steel." *ASM Source Book on Maraging Steels*, p. 37, 1979.

12. Stavros, A. J., and H. W. Paxton. "Stress-Corrosion Cracking Behavior of an 18 Pct. Ni Maraging Steel." *ASM Source Book on Maraging Steels*, p. 179, 1979.

INTENTIONALLY LEFT BLANK.

Appendix A. Qualification of Hunter Army Air Field (HAAF), Savannah, GA for Cadmium Brush Plating Rework of Shock Strut Mounts

A.1 Background

The U.S. Army Research Laboratory (ARL) was asked by the U.S. Army Aviation and Missile Command (AMCOM) to qualify Hunter Army Air Field (HAAF), Savannah, GA for cadmium brush plating rework of shock strut mount components that are removed from service due to worn vacuum cadmium coating. The information that follows was included in the trip report sent to Dr. Kirit Bhansali of AMCOM. The qualification took place 8–10 June 1997 by Marc Pepi (T.O. no. PEP3283TJ80934) and Sharad Pednekar (T.O. no. PED82102J80964). Qualification was performed by the use of three-point bend test specimens (a total of four), tested in accordance with American Society for Testing and Materials (ASTM) F519.[1] The four specimens were machined from the webbing of the failed AH-64 Landing Support Strut and cadmium brush plated by HAAF. The testing was performed to determine whether the brush plating process would embrittle this material (Maraging Grade 300 steel) under high stress (80% and 92% of the ultimate tensile strength).

A.2 Brush Plating Process and Theory

Brush plating, also known as selective plating, is a portable method of applying coatings to the localized areas of damaged work pieces and components without using an immersion tank.[2] This process is advantageous to the part under investigation in that it will minimize repair turnaround time. The process is described in general terms as follows: The operator soaks a plating tool in the plating solution. The tool has an adsorbent cloth wrapped around its anode, which is used to apply the plating solution to the work area of the part being repaired. A power supply produces the direct current necessary for the plating process to occur. Two leads coming from the power supply connect to the plating tool and the part being plated, respectively. When the tool is placed on the part, plating occurs as a result of the completed circuit. The precleaning operation is performed in a similar manner with a cleaning solution. Subsequent to cadmium brush plating, the part is dipped into a chromic acid solution to provide additional corrosion protection.

A.3 Test Plan

The thickness of each of the four specimens was measured and listed as well as the deflection in Table A-1.

---

[1] American Society for Testing and Materials. "Standard Test Method for Mechanical Hydrogen Embrittlement Evaluation of Plating Processes and Service Environments." ASTM F519, West Conshohocken, PA, 1997.

[2] Surface Finishing. "Brush Plating Applies Coatings On-Site or In-House to Repair Equipment." <www.surfacefinishing.com>, 27 October 1999.

Table A-1. Calculated thickness and deflection of HAAF specimens.

Specimen	Thickness (in)	Deflection at 80% UTS (mils)	Deflection at 92% UTS (mils)
1	0.101	NA	193
2	0.103	NA	189
3	0.101	168	NA
4	0.102	166	NA

The deflection was calculated from the following formula, listed within ASTM G39[3] for three-point bend testing. Textbook values for strength were used.

$$\sigma = \frac{6Ety}{H^2},$$

(1)

where

σ = stress,

E = Young's modulus,

t = specimen thickness,

y = deflection, and

H = distance between contact points.

The mechanical properties of Maraging Grade 300 steel are listed as follows:

UTS = 275 ksi,

YS = 270 ksi,

%El = 4%T, 8%L, and

E = 26.5 × 106 psi.

A.4 Synopsis of Essential Information

Aviation and Troop Command representatives (Mr. Randy McFarland and Mr. William Alvarez) accompanied the ARL representative (Mr. Marc Pepi and Dr. Sharad Pednekar) to HAAF. ARL had fixturing developed that would test the flat specimens (3/4 × 4 × ~0.100 in) in three-point bending per ASTM F519. Cadmium brush plating was performed by Engineering Technician John Cook of HAAF on four specimens fabricated from an AH-64 Landing Support Strut. Mr. Cook was directed to plate these specimens in the exact manner he would have plated an actual component fielded from service. Mr. Cook was certified by the LDC Corporation for plating processes involving LDC products. The brush plating method followed was LDC-4803, "Process Procedure for Preparing and Electroplating Ultra-High Strength Steel with LDC-4803 Cadmium S (Low Hydrogen Embrittlement)." Mr. Cook used a portable LDC Model 3025120-1C power supply, serial no. 1996. The cadmium solution used was clear and appeared relatively new. It had the following characteristics, as taken from the label:

---

[3] American Society for Testing and Materials. "Standard Practice for Preparation and Use of Bent-Beam Stress-Corrosion Test Specimen." ASTM G39, West Conshohocken, PA, 1999.

Type: LDC-4803, Cadmium (No Bake)
Batch: 041597
Recommended Voltage Range: 6–20 V
Plating Factor: 0.007
Manufactured: 4/1/97
Solution Embrittlement Test Date: 4/15/97.

The chromate conversion coating solution used had the following characteristics:

Type: LDC-1721, DPM 3689.
Batch: 051997
Shelf Life: Unlimited.

The first task was to unload specimen no. 3 from a test fixture, which was loaded to 92% of its UTS on Thursday, 5 June 1997. It was unloaded at ~0900 hr on 9 June 1997 and exhibited no sign of plastic deformation. The dial gauge recorded a value of −0.192 in upon removal of the load, which was consistent with the loading deflection imparted on the specimen.

The first specimen brush plated by HAAF was specimen no. 1. The specimen was immersed into a bath of 1,1,1 trichloroethane for degreasing purposes. Mr. Cook attached a cotton batting to the graphite-tipped anode and dipped it into electrocleaning solution LDC-01. The power supply was set to reverse polarity and ~12 V (10–15 V required). The current ranged from 5–10 A and varied depending upon the amount of force placed on the specimen. The part was cleaned with the solution on all sides, for a total of 0.083 A-hr. The specimen was rinsed with tap water and examined. If the water did not break, there was no film remaining, and the part was ready for plating. Further cleaning would be necessary if the water did break. The part was subsequently cadmium brush plated with the LDC-4803 solution. The voltage ranged from 11.5–13 V and the current ranged from 3.5–5 A. This process was performed using the "forward" polarity setting for a total of 0.141 A-hr on all sides of the specimen. The part was again rinsed in tap water. Mr. Cook expressed that no guideline existed, and the cadmium plating process was complete when it simply "looked" acceptable. The part was subsequently dipped (for ~1 to 2 s) into the LDC-1721 chromate solution, water rinsed, and air blasted. Again, this was performed until the part looked visually acceptable. The chromate solution was used in the undiluted state by Mr. Cook, who later agreed that the LDC specification required a dilution. Because the part was already dipped into the full-strength solution, it was determined that an 80% specimen would also be dipped into the full-strength solution. The part was placed into the test fixture and loaded to 0.193-in deflection. Specimen nos. 2–4 were prepared in a similar manner with the variables listed in Table A-2.

31

Table A-2. Specimen plating variables (HAAF).

Feature	Specimen no. 1	Specimen no. 2	Specimen no. 3	Specimen no. 4
Cleaning current (A)	5–10	5–10	5–10[a]	5–10
Cleaning voltage (V)	13.5	15	15[a]	15
Cleaning duration (A-hr)	0.083	0.087	0.090[a]	0.172
Plating current (A)	3.5–5	5–10	5–10[a]	5–10
Plating voltage (V)	11.5–13	15–18	15–18[a]	15–18
Plating duration (A-hr)	0.141	0.181	0.242[a]	0.134
Chromate solution	undiluted	diluted 50%[b]	diluted 50%[b]	undiluted
% UTS	92%	92%	80%	80%
Deflection (in)	0.193	0.189	0.168	0.166
Load start time	0915, 6/9/97	0950, 6/9/97	1008, 6/9/97	1024, 6/9/97

[a]Estimated.

[b]Diluted to 50% with tap water. Note: Item 16 of LDC solution data sheet states to dilute the solution to 4–9:1 with deionized water. This was overlooked by Mr. Cook while he performed the brush plating process.

The loaded parts were placed into a padded storage box and returned to ARL.

The plating thickness of the cadmium deposited on each specimen was estimated using the formula listed in the Tool and Manufacturing Handbook, Volume 3:[4]

$$EAH = (f)(a)(t) \tag{2}$$

where

EAH = estimated A-hr,
f = plating factor (0.007 A-hr/in^2/10^{-4} in),
a = surface area plated (in^2), and
t = thickness of plating × 1000 (i.e., t = 5 correlates to 0.0005-in-thick plating).

These calculations are estimates at best, especially for specimen no. 3, for which the EAH was estimated, rather than recorded. These thickness estimates are averages and are based on the premise that the operator evenly plated the entire specimen. The estimated plating thickness for specimen no. 1 was calculated as follows:

$$EAH = (f)(a)(t)$$
$$0.141 = (0.007)(0.75 \times 4 \times 2 + 0.75 \times 0.101 \times 2 + 4 \times 0.101 \times 2)(t)$$

➤ t = 0.00029

The estimated thicknesses were calculated in a similar manner for specimen nos. 2–4 and are listed below:

Specimen no. 1 estimated plating thickness: 0.00029 in,
Specimen no. 2 estimated plating thickness: 0.00037 in,
Specimen no. 3 estimated plating thickness: 0.00050 in, and
Specimen no. 4 estimated plating thickness: 0.00028 in.

---

[4] Society of Manufacturing Engineers. *Tool and Manufacturing Engineers Handbook.* "Materials Finishing and Coating," vol. 3, pp. 20–44, 1985.

A.5 Results of Testing

The specimens remained under load for 8 weeks at each loading without failure, and there was no sign of cracking. It was determined that HAAF was qualified to perform cadmium brush plating rework on the AH-64 Apache shock strut mount.

INTENTIONALLY LEFT BLANK.

Appendix B. Qualification of Ft. Lewis, Dupont, WA for Cadmium Brush Plating Rework of Shock Strut Mounts

B.1 Background

The U.S. Army Research Laboratory (ARL) was also asked to qualify Ft. Lewis, Dupont, WA for cadmium brush plating rework of shock strut mount components that are removed from service due to a worn vacuum cadmium coating. This would ensure that there would be a rework facility on the West coast as well as the East coast. The information that follows was included in the trip report sent to Dr. Kirit Bhansali of the U.S. Army Aviation and Missile Command (AMCOM). The qualification took place 17–18 March 1998 by Marc Pepi (T.O. no. PEP3283TE84502). Similar to Hunter Army Air Field (HAAF), qualification was performed by the use of three-point bend test specimens (a total of four), tested in accordance with American Society for Testing and Materials (ASTM) F519.[1] The four specimens were machined from the webbing of an intact AH-64 Landing Support Strut, sent to ARL from AMCOM, and cadmium brush plated by Ft. Lewis. Again, the purpose of this testing was to determine whether the brush plating process would embrittle this material (Maraging Grade 300 steel) under high stress (80% and 92% of the ultimate tensile strength).

B.2 Test Plan

Four specimens were fabricated from AH-64 Main Landing Gear Mount Part No. 1560-01-341-6213 7-311113409-2 by ARL. The specimens were three-point bend tested using the fixture shown in Figure 1b of specification ASTM G39.[2] Deflection was measured using a fixture similar to that shown in Figure 3 of that specification. The deflection was calculated from the following formula, in accordance with ASTM G39 guidelines:

$$\sigma = \frac{6Ety}{H^2},$$ (1)

where

$\sigma =$ stress,
$E =$ Young's modulus,
$t =$ specimen thickness,
$y =$ deflection, and
$H =$ distance between contact points.

Table B-1 lists the calculated deflection based on converted Rockwell hardness values and specimen thickness. Hardness testing was used rather than textbook values for strength.

---

[1] American Society for Testing and Materials. "Standard Test Method for Mechanical Hydrogen Embrittlement Evaluation of Plating Processes and Service Environments." ASTM F519, West Conshohocken, PA, 1997.

[2] American Society for Testing and Materials. "Standard Practice for Preparation and Use of Bent-Beam, Stress Corrosion Test Specimens." ASTM G39, West Conshohocken, PA, pp. 1–7, 1994.

Table B-1. Calculated thickness and deflection of Ft. Lewis specimens.

Specimen	Thickness (in)	Hardness (Avg. of 4) HRC	Converted UTS (ksi)	Stress Level (%)	Deflection (mils)
1	0.101	52.8	281	80	175
2	0.103	51.7	270	80	168
3	0.101	52.3	276	92	202
4	0.102	51.6	269	92	192

B.3 Synopsis of Essential Information—Plated Specimens

Cadmium brush plating was performed by Mr. Brian Norling of Ft. Lewis. Mr. Norling was directed to plate these specimens in the exact manner he would have plated an actual component fielded from service. Mr. Norling was not certified to perform brush plating, but was trained by certified personnel. The brush plating method followed was a SIFCO* document entitled, "Plating With Cadmium Code 2023 Solution." The specimens were first electrocleaned using the LDC Corporation Electroclean -01, with a required voltage range of 10–15 V. The cadmium solution used the was SIFCO Code 5070, which has recently replaced SIFCO Code 2023 (each solution has the same Federal Stock Number). Although Ft. Lewis did not possess the procedure sheet for the Code 5070 solution, ARL was assured that the procedure was the same for the Code 2023 solution. The Code 5070 solution appeared fresh and clear, and had the following characteristics:

Type: SIFCO Cadmium LHE Code SPS 5070
Batch: 9605014
Recommended Voltage Range: 6–12 V small, 8–20 V large
Plating Factor: 0.007
Manufactured: 5/2/96
Tested for Embrittlement: Yes (no date or material listed).

Ft. Lewis had two chromate conversion solutions. The representative characteristics are listed below:

Manufacturer: LDC Corporation
Type: LDC-1721, DPM-3689
Batch: 051997
Shelf Life: Unlimited.

Manufacturer: SIFCO
Type: SIFCO Code 5005
Batch: Not Listed
Shelf Life: Unlimited.

Mr. Norling used a portable SIFCO Power Supply, Model CP60-25-115-1, S/N 92024 for brush plating. The number of amp-hours necessary to deposit ~0.0003 in of cadmium was calculated

---

* SIFCO, 5708 Schaaf Road, Cleveland, OH 44131.

prior to plating. The four specimens were then degreased using toluene in accordance with TT-T-548E, and a cheesecloth swab. Mr. Norling had prepared two graphite anodes with cotton batting overlays one each for the electroclean solution and the cadmium solution. After the specimens were degreased, they were electrocleaned using the LDC-01 solution with the power supply on reverse polarity. The specimen was swabbed on the faces, and not the edges. The edges were coated by the throwing power of the anode. A voltage of ~10–11 V was used for up to 0.0911 A-hr. The electrocleaned specimens were rinsed with tap water, and tested for water break. If the water did not break, the samples were prewet with the Code 5070 cadmium solution and the power supply was set to forward polarity. A plating voltage of 6–9 V was used (SIFCO recommends 9 V, maximum, to avoid burning the specimen) for ~0.2000 A-hr. After plating, the specimens were rinsed with tap water and tested for water break. If the water did not break, the specimens were blown dry using compressed air. The specimens were then buffed using a ScotchBrite* pad (Type A, Very Fine), applying no pressure. The LDC Code 1721 solution was diluted 4:1 with deionized water (4–9:1 requirement) prior to use and placed into a shallow container. The specimens were dipped into the solution for ~2 s, or for as much time as was needed to produce a dark gold, uniform coating. Blotched areas were touched up by swabbing additional solution. Specimen 1 was mistakenly left in the solution for ~10 s. Table B-2 lists the variables for each specimen.

Table B-2. Specimen plating variables (Ft. Lewis).

Feature	Specimen no. 1	Specimen no. 2	Specimen no. 3	Specimen no. 4
Cleaning voltage (V)	10.4	10.7	11.2	11.2
Cleaning current (A)	6.6 max.	8.1 max.	8.6 max.	9.7
Cleaning duration (A-hr)	0.0697	0.0657	0.0504	0.0911
Plating voltage (V)	6.4 and 7.4	6.5 and 7.4	6.5 and 7.4 and 8.0 and 8.8	6.8 and 7.8 and 8.2 and 8.8
Plating current (A)	3.0 max.	3.3 max.	4.9 max.	4.9 max.
Plating duration (A-hr)	0.1307	0.1231	0.1240	0.1260
Total (A-hr)	0.2004	0.1888	0.1744	0.2171
Chromate solution	4:1, 10 s	4:1, 4 s	4:1, 2 s (touchup = 2 s)	4:1, 2 s
% UTS	80%	80%	92%	92%
Deflection (in)	0.175	0.168	0.202	0.192
Load Date	3/17/98	3/17/98	3/17/98	3/17/98

Specimen 4 was cleaned with denatured alcohol prior to the chromate treatment in an effort to reduce the blotching noticed on the first three specimens. It was believed that the blotches might have been caused by oil that was in the compressed air line. Mr. Norling created a condensed procedure sheet for the specimens. The loaded specimens were placed into a padded storage box and returned to ARL for monitoring. As with HAAF, the plating thickness of the cadmium deposited on each specimen was estimated using the formula listed on pp. 20–44 of the Tool and Manufacturing Handbook, Volume 3.[3]

---

* ScotchBrite is a registered trademark of the 3M Company.

[3] Society of Manufacturing Engineers. *Tool and Manufacturing Engineers Handbook*. "Materials Finishing and Coating,"

$$EAH = (f)(a)(t), \tag{2}$$

where

EAH = estimated amp hours (A-hr),
f = plating factor (0.007 A-hr/in^2/10^{-4} in),
a = surface area plated (in^2), and
t = thickness of plating × 1000 (i.e., t = 5 correlates to 0.0005-in-thick plating).

These thickness estimates are averages and are based on the premise that the operator evenly plated the entire specimen. The estimated plating thickness for specimen no. 1 was calculated as follows:

$$EAH = (f)(a)(t)$$

$$0.1307 = (0.007)(0.75 \times 4 \times 2)(t) \tag{3}$$

$$\longrightarrow t = 0.00031 \text{ in.}$$

The estimated thicknesses were calculated in a similar manner for specimen nos. 2–4, and are listed as follows:

Specimen no. 1 estimated plating thickness: 0.00031 in,
Specimen no. 2 estimated plating thickness: 0.00029 in,
Specimen no. 3 estimated plating thickness: 0.00030 in, and
Specimen no. 4 estimated plating thickness: 0.00030 in.

The estimated thicknesses indicate that the Ft. Lewis brush plating procedure is highly controlled and repeatable because a cadmium coating thickness of 0.0003 in was sought.

B.4 Synopsis of Essential Information—Plated Strut Mount

Ft. Lewis was subsequently directed to brush plate an actual component that was in inventory. The component had been taken out of service due to a large radius crack. The process was optimized by trying various methods. Initially, the part was placed into a SIFCO Turning Head apparatus, but the weight imbalance of the part and the delicate nature of the grip prohibited the required pressure from being applied to the part by the anode. This led to an uncoated radius (where cracking initiates in the field), as evidenced by the inability of the chromate solution to react at this region. It was determined that the part would be plated by turning the part by hand on the tabletop. This would allow the pressure necessary to coat the radius. Mr. Norling grit blasted the area of concern (1.75-in radius) with aluminum oxide and wiped the region with toluene. The part was prewet with the preclean solution, then precleaned in reverse polarity at 11.1 V for 0.0192 A-hr. The part was rinsed with tap water (water break test) and plated at 7.0, 7.5, 8.0, and 9.0 V for a total of 0.02518 A-hr (0.2501 A-hr was the goal for a coating thickness of 0.0003 in). The part was subjected to the water break test again, and air dried. The part was hand buffed with a very fine ScotchBrite pad and chromated for 2 s by dipping in the LDS solution diluted to 4:1. The area around the radius (which did not receive adequate cadmium coverage while the part was in the SIFCO Turning Head) was determined to have ample cadmium using this method. This may have been because the operator could exert more pressure

38

with the rectangular graphite anode as opposed to the Turning Head method where the radius was perpendicular to the table. It was determined that the SIFCO chromate solution resulted in a more uniform and aesthetically pleasing finish than the LDS chromate solution. The part was subsequently air dried, and Mr. Norling recorded the condensed procedure onto a Dalic Process Procedure form. The estimated plating thickness for this part was consistent with the goal of a 0.0003-in-thick coating and was calculated as follows:

$$EAH = (f)(a)(t)$$

$$0.2518 = (0.007)(12.35)*(t) \tag{4}$$

$$\longrightarrow t = 0.00029 \text{ in}$$

* = the area was calculated as not only the cylindrical region, but also the base that comes into contact with the anode. The area of the base was calculated to be:

$$a = \pi/4(D^2-d^2), \tag{5}$$

where

D = 2.375 in,
d = 1.75 in, and
a = 2.02 in.

The area of the cylinder was calculated as follows:

$$a = 2\pi rh, \tag{6}$$

where

r = 0.875 in,
h = 1.88 in, and
a = 10.33 in^2.

After the part was plated, it was magnetic particle inspected to determine whether the plating would mask the discontinuity. The part was subjected to 2000 A for a split second and sprayed with fluorescent particles. The discontinuity was revealed as a result of this inspection.

B.5 Test Results

The specimens remained under load for 8 weeks at the respective loads. It was determined that HAAF was qualified to perform cadmium brush plating rework on the AH-64 Apache shock strut mount. ARL furnished Ft. Lewis a procedure sheet to be used while plating the actual main landing gear mounts, which is included on the following page:

AMCOM-APPROVED PROCEDURE FOR PREPARING AND CADMIUM BRUSH PLATING AH-64 MAIN LANDING GEAR MOUNTS AT FT. LEWIS, WASHINGTON, 8 APRIL 1998

1. Preclean the part. Degrease with a non-flammable solvent. Remove any oxides, corrosion, scale or any organic coatings by lightly blasting with aluminum oxide media. Be careful not to damage threads with grit blast. Clean off grit blasted region with nonflammable solvent.

2. Prepare 2-in × 3-in graphite anode with cotton batting, and soak in LDC-01 solution. Prepare another 2-in × 3-in graphite anode and soak in SIFCO 5070 LHE cadmium solution.

3. Prewet the area to be plated with LDC-01 solution.

4. Electroclean with LDC-01 Reverse (Negative) polarity at 10-15 V, for ~0.05 A-hr.

5. Water rinse thoroughly with clean tap water. Check to make sure no water breaks occur.

6. Air dry part with filtered compressed air.

7. Prewet part with SIFCO 5070 LHE cadmium solution.

8. Brush plate with SIFCO 5070 LHE cadmium Forward (Positive) polarity at 6–9 V for ~0.2501 A-hr (for a coating thickness of 0.0003 in). Do not exceed 9 V.

9. Water rinse thoroughly with clean tap water. Check to make sure no water breaks occur.

10. Air dry part with filtered compressed air.

11. Hand buff coated region lightly (apply no pressure) with Type A "Very-Fine" ScotchBrite pad.

12. Dip or swab coated region in LDC-1721 or SIFCO 5005 chromate solution. The LDC solution must be diluted 4-9:1, while the SIFCO product is used as-is. Chromate solution should be kept on part for only about 2 s, or until a uniform dark gold coating results. Ensure radius is adequately chromated. Radius and spotty areas may be retouched by swabbing chromate solution.

13. Rinse off chromate solution in water.

NOTES:

1. Use a different anode for precleaning and plating process.

2. If radius does not react to chromate solution, it is most likely not plated. Part must be replated (repeat steps 1–13).

Appendix C. Salt Fog Testing of Cadmium Brush Plated Specimens From Hunter Army Air Field (HAAF) and Ft. Lewis

C.1 Background

The U.S. Army Aviation and Missile Command (AMCOM) requested the qualification of two facilities for the cadmium brush plating of AH-64 landing support struts (shown in Figure C-1). The facilities would perform rework in the spindle to webbing radius that has been the origin of many failures over the past decade. As part of the qualification process, the U.S. Army Research Laboratory (ARL) performed hydrogen embrittlement testing on specimens that were cadmium brush plated by the Hunter Army Air Field (HAAF), Savannah, GA, and Ft. Lewis, WA. Each facility used a "no-bake," non-embrittling solution for plating. The specimens were produced in accordance with American Society for Testing and Materials (ASTM) G39[1] from two separate AH-64 Landing Support Struts comprised of Maraging 300 Grade steel. Each specimen withstood 8 weeks of ambient exposure (75 °F and 50% relative humidity) at 80% and 92% ultimate tensile strength (UTS) loading without failure. Based upon the results of ambient loading, the two facilities were qualified to perform cadmium brush plating operations.
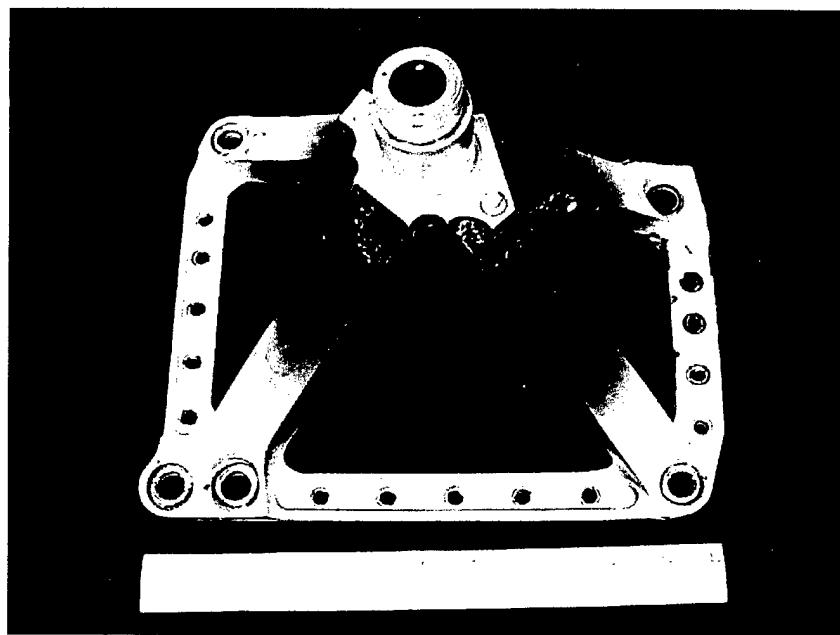
Figure C-1. Intact shock strut mount shown in the as-received condition (reduced 75%).

---

[1] American Society for Testing and Materials. "Standard Practice for Preparation and Use of Bent-Beam, Stress Corrosion Test Specimens." ASTM G39, West Conshohocken, PA, pp. 1–7, 1994.

After hydrogen embrittlement testing was completed, the specimens were unloaded and subjected to salt fog exposure while reloaded to 75% and 90% of the yield strength. This testing was performed in order to gain an understanding of how these coatings would behave in a stress corrosion cracking (SCC) environment and to provide exposure data for these two stress levels.

C.2 Salt Fog Testing

Salt fog testing was conducted in accordance with ASTM B117.[2] A sodium chloride level of 5% was used for all testing. Table C-1 contains the results of salt fog testing of the specimens that were brush plated at HAAF. One of the HAAF specimens was loaded to 90% yield strength while another was loaded to 75% yield strength. The specimens were loaded into the fixtures shown in Figure C-2. The final specimen was not plated, and loaded to 90% yield strength. As anticipated, the unplated specimen was the first to fail, followed by the 90% loaded specimen, then finally, the 75% loaded specimen.

Table C-1. Results of salt fog testing of HAAF brush-plated specimens.

Specimen	Prior History	ARL Salt Fog Testing	Deflection (in)	Salt Fog Duration to Failure (hr)[a]	Comments
1	Cadmium brush plated, loaded to 92% UTS at HAAF	Loaded to 90% YS, placed into salt fog	0.182	428–492	White corrosion products and some rusting at the contact points. Some base metal exposed.
2	Cadmium brush plated, loaded to 80% UTS at HAAF	Loaded to 75% YS, placed into salt fog	0.154	1495–1510.5	Rust of base metal on tensile side, white corrosion products on compressive side
3	Unplated/unloaded	Loaded to 90% YS, placed into salt fog	0.208	124.5–143.5	~95% of entire surface contained general corrosion

[a] Hours are estimated because continuous monitoring was not feasible (failed overnight or weekend).
Note: YS = yield strength.

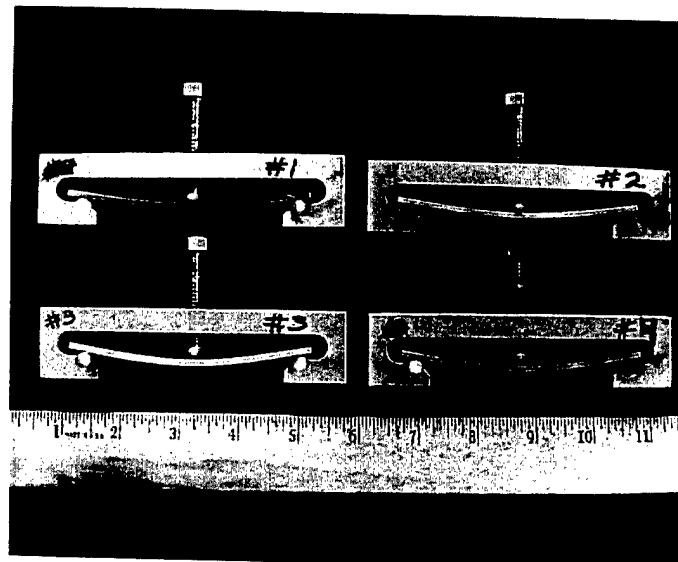Figure C-2. Fixtures used for the stress corrosion testing of bent beam specimens (reduced 64%).

---

[2] American Society for Testing and Materials. "Standard Practice for Operating Salt Spray (Fog) Apparatus." ASTM B117, West Conshohocken, PA, 1997.

Table C-2 lists the results of salt fog testing of the specimens that were brush plated at Ft. Lewis. A total of two Ft. Lewis specimens were loaded to 90% yield strength while the remaining two were loaded to 75% yield strength.

Table C-2. Results of salt fog testing of Ft. Lewis brush-plated specimens.

Specimen	Prior History	Salt Fog Testing	Deflection (in)	Salt Fog Duration to Failure (hr)[a]	Comments
1	Cadmium brush plated, loaded to 80% UTS at Ft. Lewis	Unloaded after 8 weeks, then loaded to 75% YS, placed into salt fog	0.158	5671.5–5766	Evidence of base metal corrosion (red rust ~40% of entire surface) as well as, greenish streaking.
2	Cadmium brush plated, loaded to 80% UTS at Ft. Lewis	Unloaded after 8 weeks, then loaded to 75% YS, placed into salt fog	0.158	7133.5–7248	Tension side exhibited almost 100% base metal corrosion (red rust) with greenish streaking. Compressive side exhibited ~40% corrosion.
3	Cadmium brush plated, loaded to 92% UTS at Ft. Lewis	Unloaded after 8 weeks, then loaded to 90% YS, placed into salt fog	0.193	2976–3051.5	Tension side exhibited almost 100% base metal corrosion (red rust) with greenish streaking. Compressive side exhibited ~40% corrosion.
4	Cadmium brush plated, loaded to 92% UTS at Ft. Lewis	Unloaded after 8 weeks, then loaded to 90% YS, placed into salt fog	0.189	4320–4393	Tension side exhibited almost 100% base metal corrosion (red rust) with greenish streaking. Compressive side exhibited ~40% corrosion.

[a] Range is provided since continuous monitoring was not feasible (failed overnight or weekend).

Because the time-to-failure for the Ft. Lewis specimens drastically surpassed that of the HAAF specimens, the chemical composition of the HAAF vs. the Ft. Lewis specimens was investigated, as well as the hardness, cadmium-coating thickness, grain size, and the fracture morphology.

C.3 Chemical Analysis

A section of each of the shock strut mounts used for specimen fabrication was analyzed in order to determine the chemical composition. The composition was determined by the Leco combustion method (carbon and sulfur) and inductively coupled argon plasma emission spectroscopy (remainder of elements). The HAAF material exceeded the requirements for nickel as listed in Boeing Mesa Specification HMS 6-1081 (Table C-3), while the Ft. Lewis material exceeded the requirements for nickel and cobalt. These levels were verified with rechecks.

Table C-3. Chemical composition (weight percent).

Element	HAAF Component	Ft. Lewis Component	HMS 6-1081
Carbon	0.02	0.03	0.03 max.
Nickel	19.55, 19.18[a]	19.32, 19.30[a]	18.0–19.0
Cobalt	9.34	9.77, 9.73[a]	8.5–9.5
Molybdenum	4.94	4.94	4.6–5.2
Titanium	0.67	0.66	0.50–0.80
Aluminum	0.15	0.16	0.05–0.15
Copper	0.15	0.11	0.25 max.
Tungsten	0.10	0.08	0.25 max.
Chromium	0.17	0.14	0.25 max.
Manganese	0.01	0.01	0.10 max.
Silicon	0.07	0.06	0.10 max.
Phosphorus	0.005	0.007	0.010 max.
Sulfur	<0.005	<0.005	0.010 max.
Zirconium	<0.005	<0.005	0.020 max.
Boron	0.0025	0.0025	0.003 max.
Calcium	<0.005	<0.005	0.050 max.
Iron	remainder	remainder	remainder

[a] Recheck value.

C.4 Hardness Testing

Rockwell hardness tests were conducted on a representative HAAF specimen, as well as a representative Ft. Lewis specimen. The "C" scale was used, which uses a 150-kg major load. The results of this testing are included in Table C-4. No significant difference in hardness was noted.

Table C-4. Results of Hardness Testing Rockwell C Scale, 150 kg.

HAAF Component (in)	Ft. Lewis Component (in)
53.3	52.6
53.5	53.2
53.6	53.2
53.3	52.8
53.4	53.7
53.3	53.1
54.1	54.1
53.4	53.6
53.6	53.4
53.9	53.2
Avg. 53.5	Avg. 53.3

C.5 Cadmium-Coating Thickness

The thickness of the brush cadmium coating and subsequent chromate treatment was analyzed to determine whether this had a role in the difference in time-to-failures. The coating thickness on each of the HAAF specimens and the four Ft. Lewis specimens were theoretically calculated

prior to salt fog testing (see qualification reports and Table C-5). As listed, the coating thicknesses of the HAAF specimens were similar to those of the Ft. Lewis specimens, with the exception of the HAAF specimen that measured 0.00050 in.

Table C-5. Theoretical cadmium plating thickness of HAAF and Ft. Lewis specimens.

HAAF Components (in)	Ft. Lewis Components (in)
0.00029	0.00031
0.00037	0.00029
0.00050	0.00030
0.00028	0.00030

C.6 Metallography

Representative SCC specimens coated by HAAF and Ft. Lewis were sectioned in order that a metallographic examination could be performed. Transverse and longitudinal samples were polished then etched with Marble's Reagent (4-g $CuSO_4$, 20-mL HCl, and 20-mL deionized water). The structure was similar in both orientations, consisting of an aged, low-carbon martensite. In addition, the material was fairly clean, exhibiting no gross defects or inclusions. Paragraph 3.4.1.3 of specification HMS 6-1081 requires a grain size of no. 7 or finer with an occasional no. 5 unless otherwise specified for material up to 3-inches in diameter or square. The grain size was determined using a metallograph with grain size reticle conforming to ASTM E112.[3] It was determined that the grain size was between ASTM nos. 6 and 7 at 100× magnification for both the HAAF and the Ft. Lewis specimens (Figures C-3 and C-4), and no appreciable difference existed between the two.
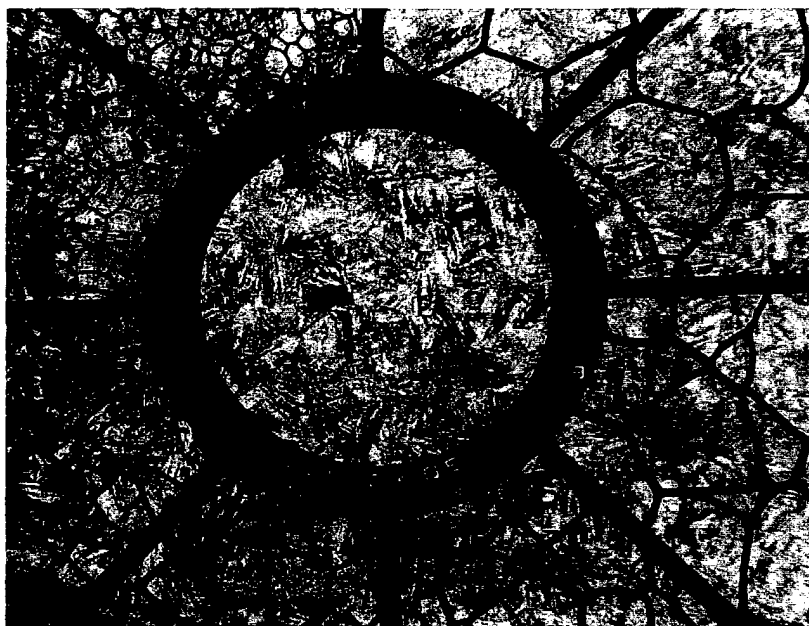

Figure C-3. Grain size of a representative HAAF specimen (mag. 100×).

---

[3] American Society for Testing and Materials. "Standard Test Methods for Determining Average Grain Size." ASTM E112, West Conshohocken, PA, 1996.
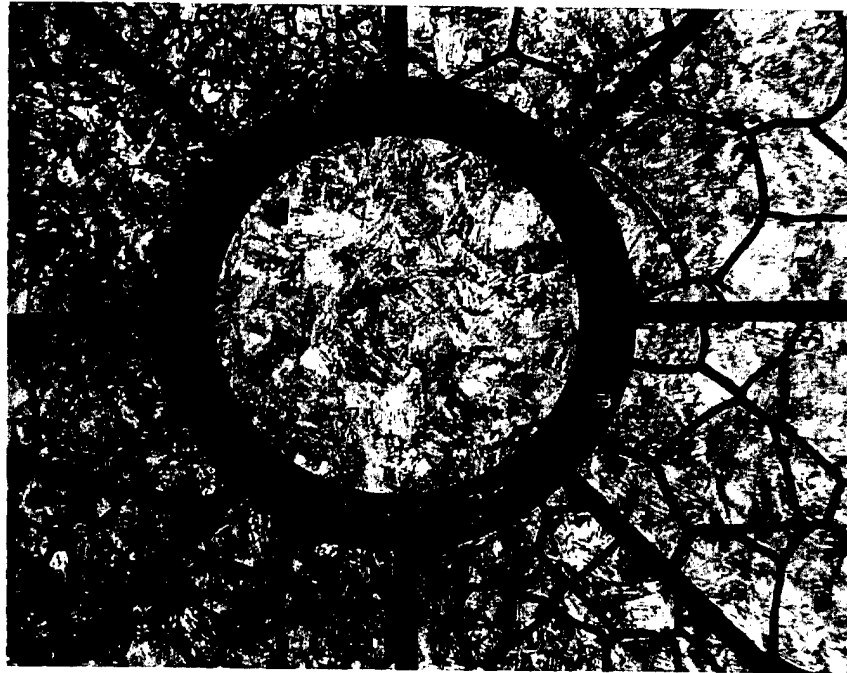
Figure C-4. Grain size of a representative Ft. Lewis specimen (mag. 100×).

C.7 Scanning Electron Microscopy (SEM)

The broken specimens were subjected to SEM to characterize the fracture morphology. The corrosion on the fracture surfaces was cleaned ultrasonically in a solution of (Brainerd Chemical) Rodine 213 (inhibited HCl). This product has been shown not to attack steel, as concentrated HCl would. The montage in Figure C-5 shows a typical fracture surface of a HAAF failed specimen. As the schematic map of the HAAF specimen illustrates (Figure C-6), the fracture surface was ~75% intergranular (Figure C-7), while the remaining surface consisted mainly of ductile dimples (Figure C-8). The fracture surface consisted of one plane and had the appearance of a brittle fracture. It was very difficult to pinpoint the exact location of the origin(s) on the fracture surface of this specimen.

Figure C-9 contains a montage of a typical Ft. Lewis failure, while Figure C-10 contains the accompanying schematic map. The fracture surfaces of the broken Ft. Lewis specimens consisted primarily of a transgranular, quasi-cleavage morphology (Figure C-11). The fracture of one of the specimens consisted of two planes with three distinct origins on the tensile side of the specimen and had the appearance of a ductile fracture. The surface was predominantly transgranular with evidence of intergranular attack and secondary cracking only at each of the three origins. Ductile dimples were noted on the compressive side of the specimen, which was the last to fail. Figures C-12 through C-14 represent the three origins at 100× magnification, while Figures C-15 through C-17 show the origins at higher magnification (200×). Figure C-18 represents the morphology noted within the center of the specimen (mixed mode; ductile and transgranular) as illustrated in Figure C-10, while Figure C-19 represents the morphology of near the compressive side of the specimen. Figure C-20 is a high-magnification scanning electron micrograph representing the ductile region (final fast fracture) on the fracture surface.

46
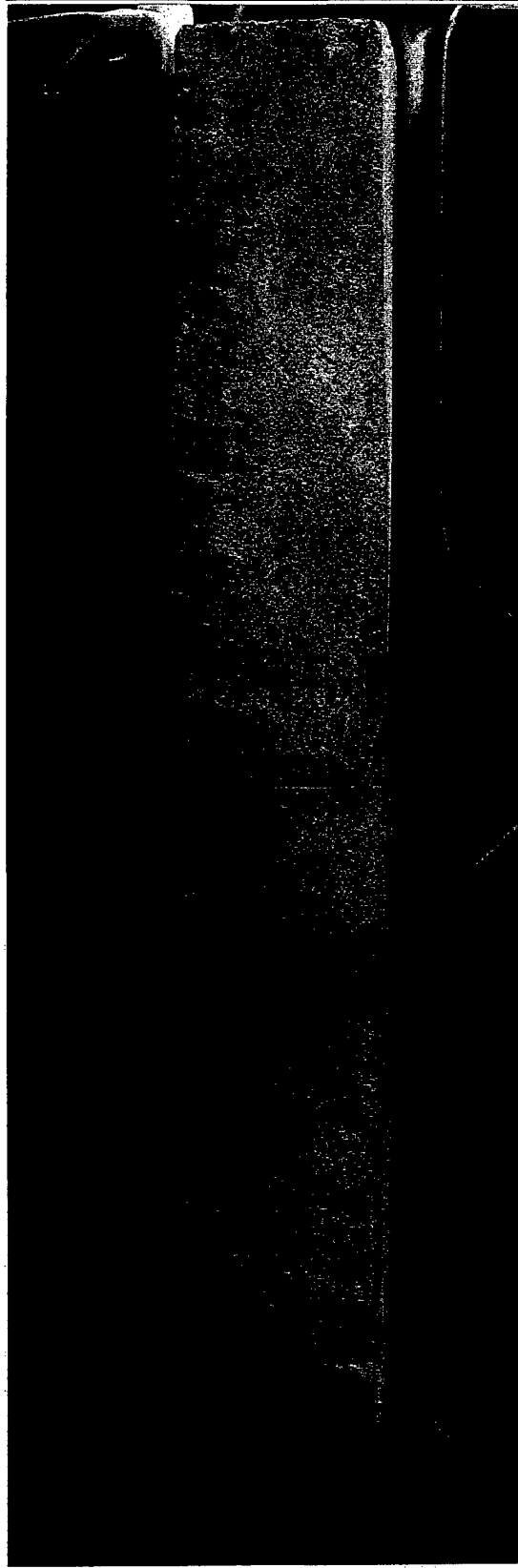
Figure C-5. Montage of a typical fracture surface of a HAAF specimen (specimen no. 1) (mag. 12×).

primarily ductile

8

7

intergranular with secondary cracking
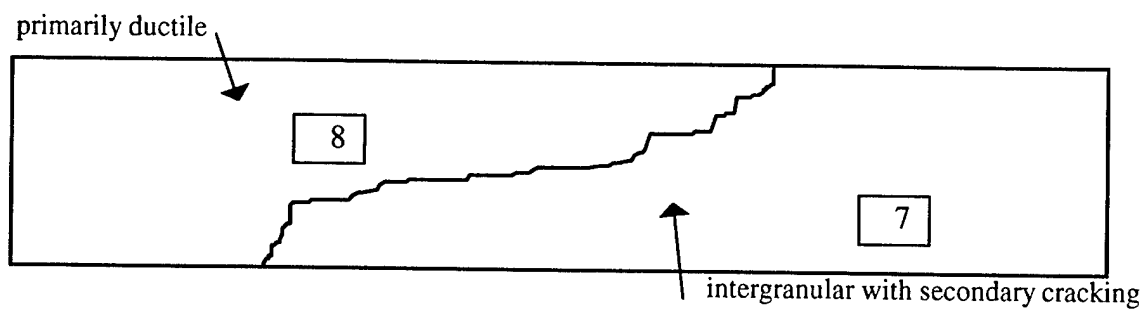
Figure C-6. Schematic illustrating a mapping of the fractographic features of the surface shown in Figure C-5. Boxes show locations of Figures C-7 and C-8.
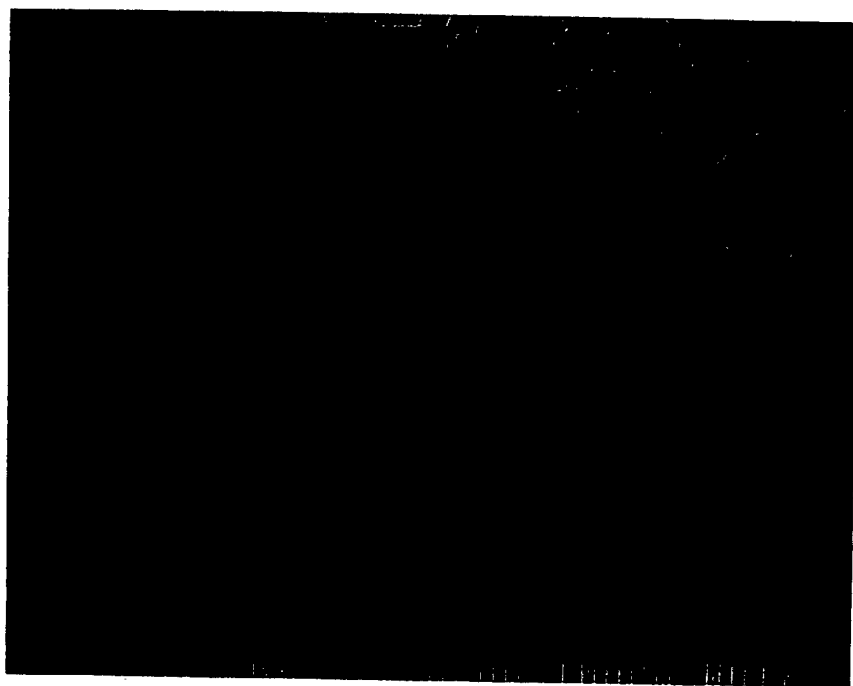
Figure C-7. Intergranular morphology prevalent on the HAAF specimens, indicative of a brittle fracture (mag. 200×).
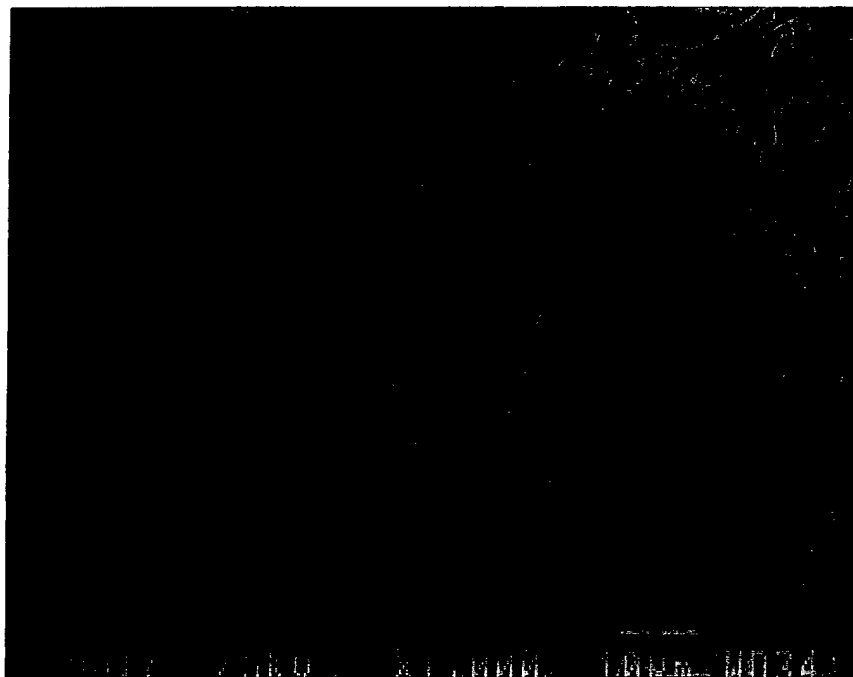
Figure C-8. Ductile morphology noted on the HAAF specimens, indicative of final fast fracture (mag. 1000×).
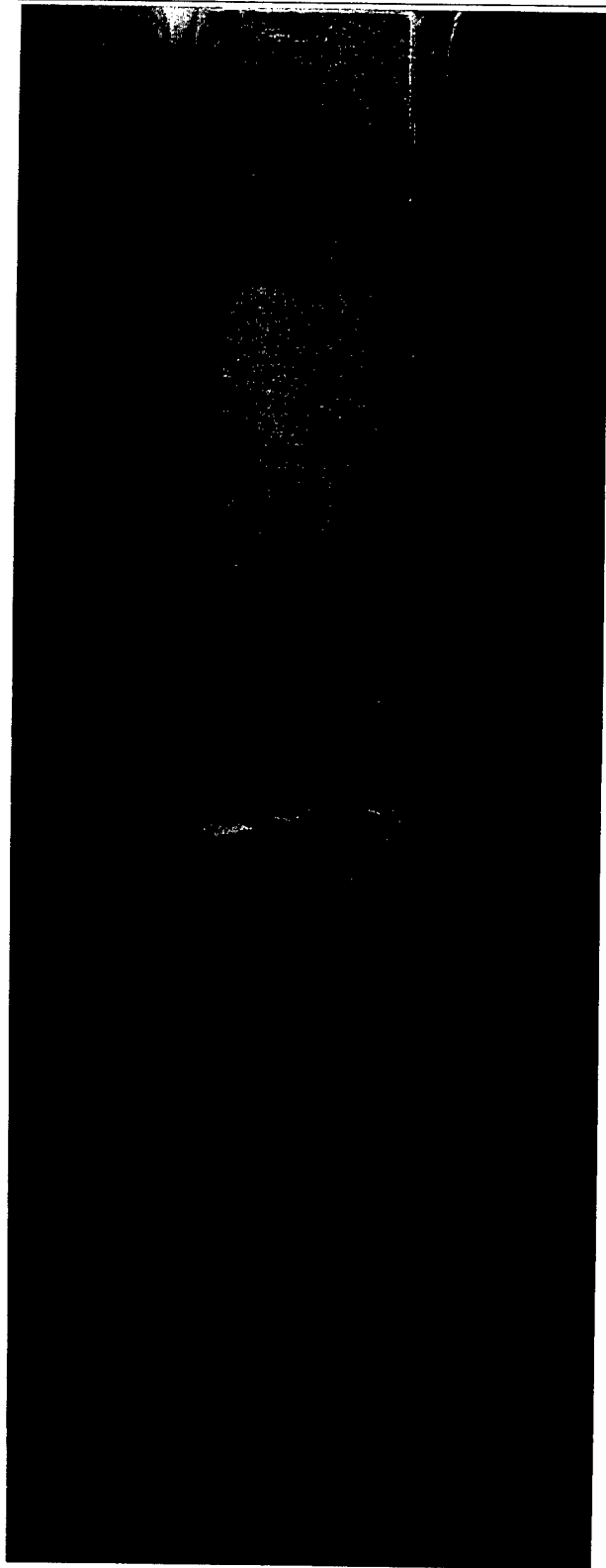
Figure C-9. Montage of a typical fracture surface of a Ft. Lewis specimen (specimen no. 3) (mag. 12×).
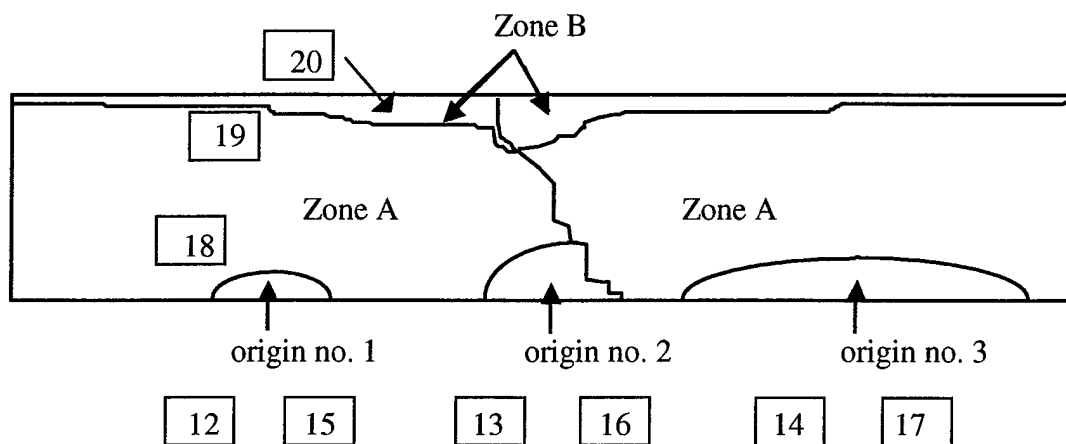
Figure C-10. Schematic illustrating a mapping of the fractographic features of the surface shown in Figure C-9. Boxes represent location of figures.

Figure C-11. Transgranular fracture morphology prevalent on the Ft. Lewis specimens (mag. 500×).
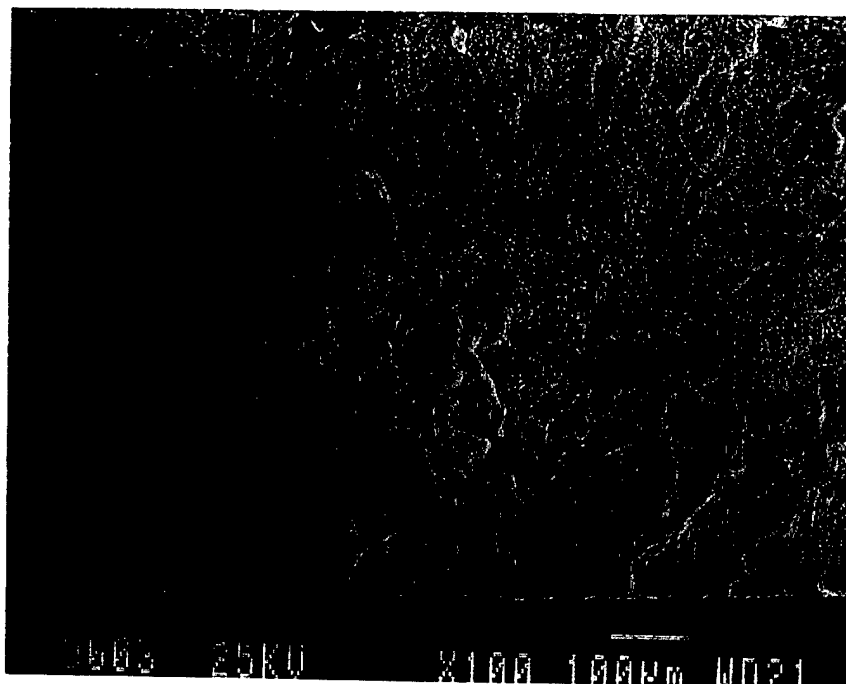
Figure C-12. Intergranular attack noted at origin no. 1 of Ft. Lewis specimen
no. 3 (mag. 100×).
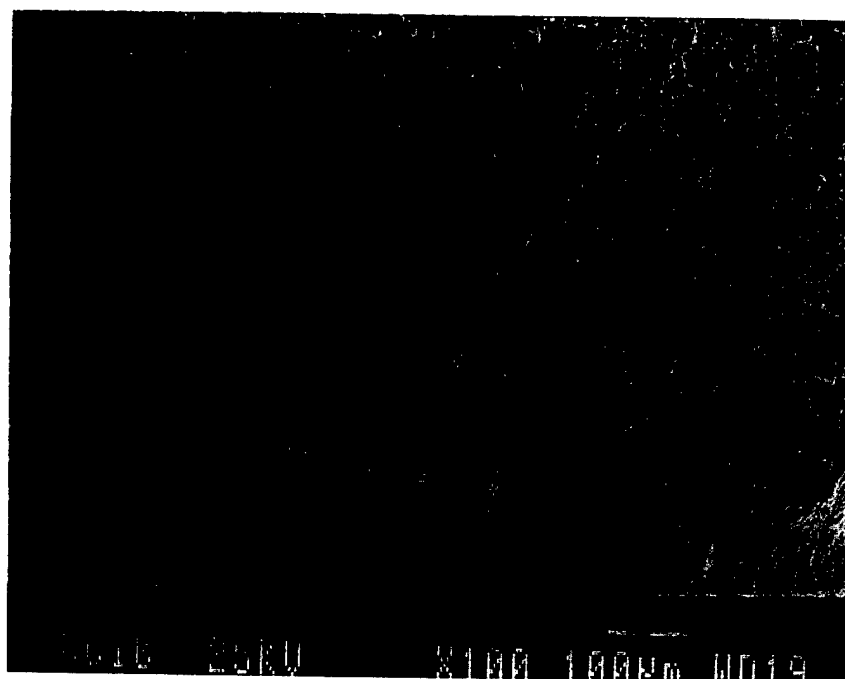
Figure C-13. Intergranular attack noted at origin no. 2 of Ft. Lewis specimen
no. 3 (mag. 100×).
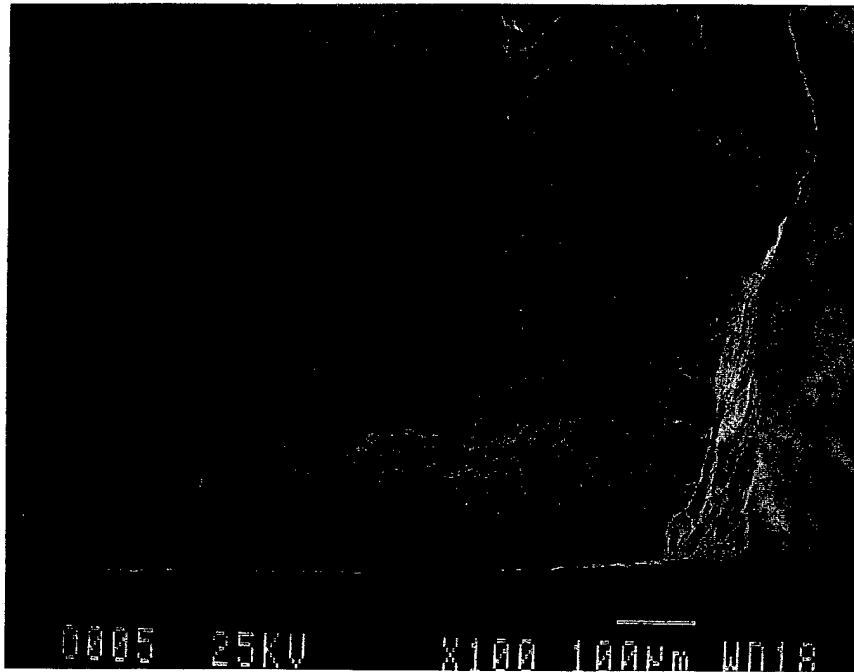
Figure C-14. Intergranular attack noted at origin no. 3 of Ft. Lewis specimen no. 3 (mag. 200×).
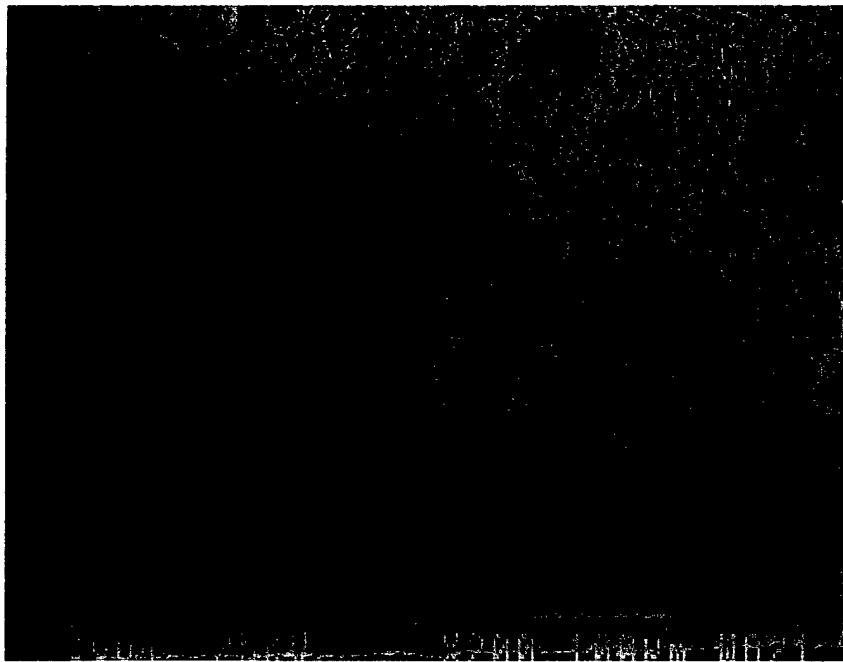
Figure C-15. Higher magnification of the intergranular attack noted at origin no. 1 (Figure C-12) of Ft. Lewis specimen no. 3 (mag. 200×).
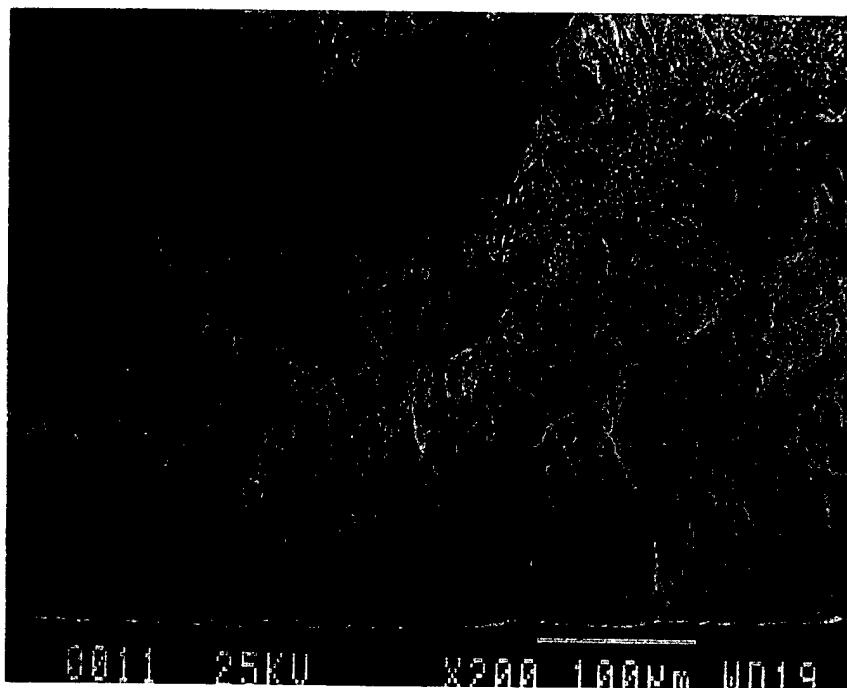
Figure C-16. Higher magnification of the intergranular attack noted at origin
no. 2 (Figure C-13) of Ft. Lewis specimen no. 3 (mag. 200×).
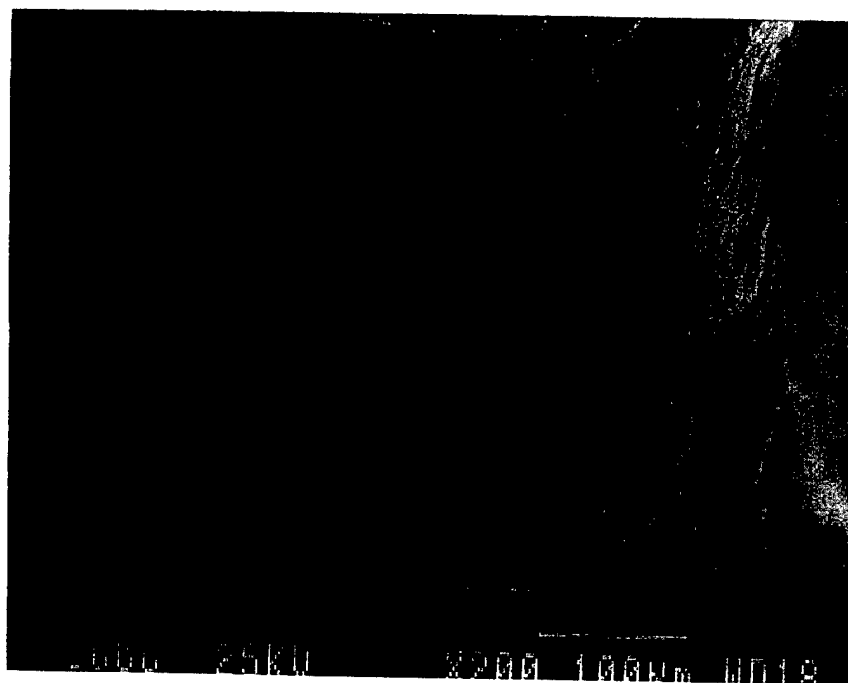
Figure C-17. Higher magnification of the intergranular attack noted at origin
no. 3 (Figure C-14) of Ft. Lewis specimen no. 3 (mag. 200×).
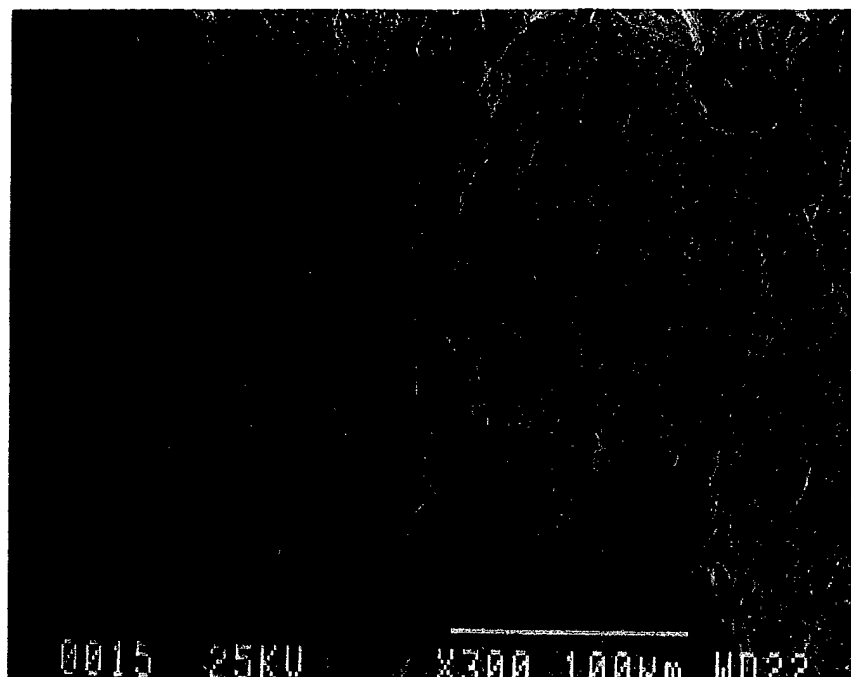
Figure C-18. Mixed mode morphology (intergranular and transgranular) noted close to origins within zone A Ft. Lewis specimen no. 3 (see Figure C-10) (mag. 300×).
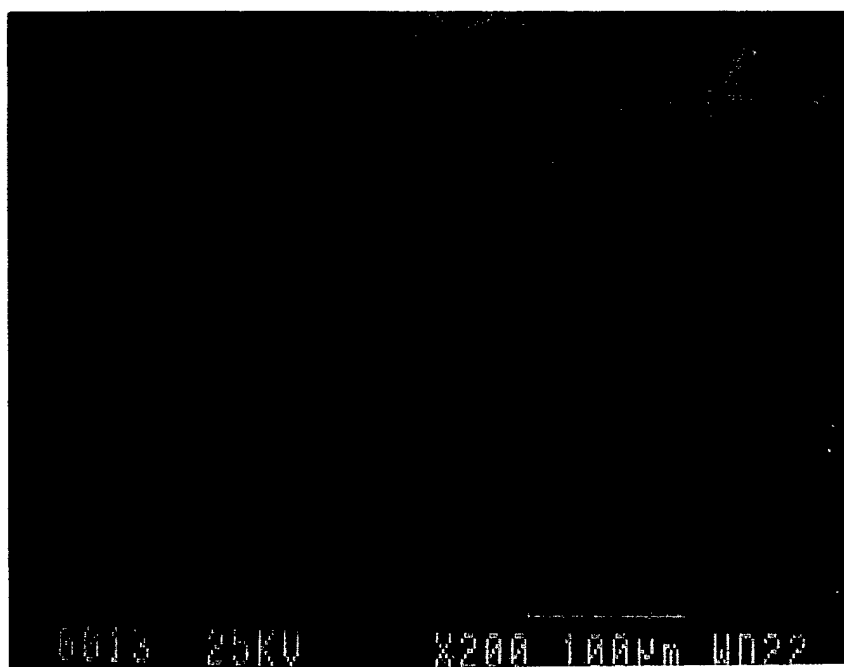
Figure C-19. Morphology noted further from origins (closer to final fast fracture region) within zone A Ft. Lewis specimen no. 3 (see Figure C-10) (mag. 200×).
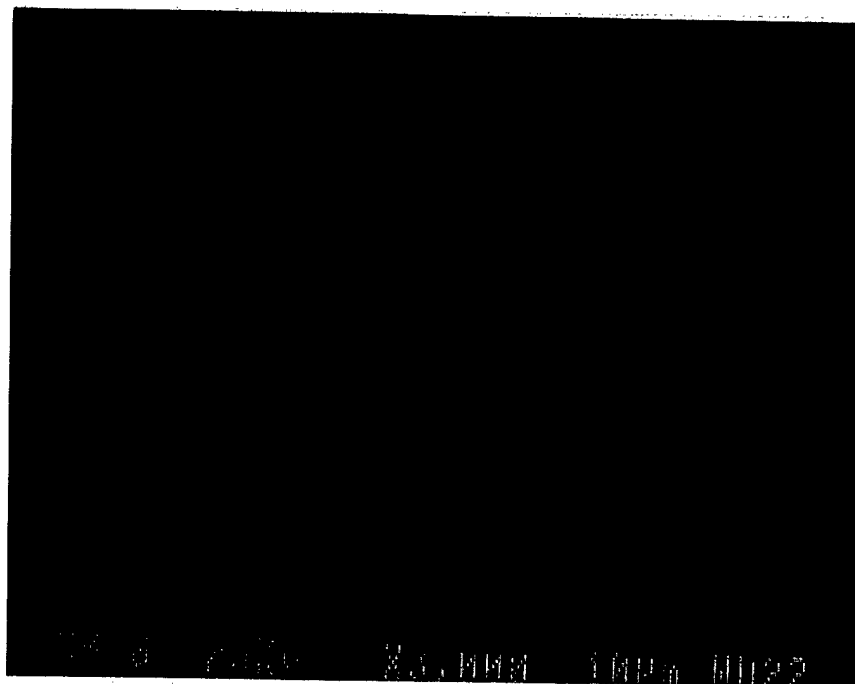
Figure C-20. Ductile morphology observed in the final fast fracture region
(zone B) of Ft. Lewis specimen no. 3 (see Figure C-10)
(mag. 200x).

C.8 Discussion

C.8.1 Fracture Path

The fracture paths of the HAAF specimens were all intergranular, while those of the Ft. Lewis specimens were each mostly transgranular. This was puzzling because the specimens were fabricated from the same location on actual components used in service that were required to conform to the same specifications, machined to the same dimensions at the same facility (ARL), and coated using similar chemicals to similar thicknesses. In addition, each specimen passed the hydrogen embrittlement test of eight weeks (suggesting the hydrogen content within the steel as a result of the coating process was of no concern), and the salt fog testing and fixturing was the same for each specimen. A survey of open literature revealed that it has been demonstrated that the fracture path of a 300 grade maraging steel can travel either in an intergranular or transgranular mode. Most references[4, 5, 6] indicate that the fracture path is almost always intergranular, while

[4] Stavros, A. J., and H. W. Paxton. "Stress-Corrosion Cracking Behavior of an 18% Ni Maraging Steel." *Metallurgical Transactions*, vol. 1, no. 11, pp. 1, 5, 7, 9, 10, 12, 13, 17, April 1970.

[5] Dean, W., and H. R. Copson. "Stress Corrosion Behavior of Maraging Nickel Steels in Natural Environments." *Proceedings of 20th Annual Conference of the National Association of Corrosion Engineers*, pp. 95, 101–103, 9–13 March 1964.

[6] Dautovich, D. P., and S. Floreen. "The Stress Corrosion and Hydrogen Embrittlement Behavior of Maraging Steels." *Proceedings of the Stress Corrosion Cracking and Hydrogen Embrittlement of Iron Base Alloys Conference*, pp. 798–799, 801–804, 810, 812, 12–16 June 1973.

transgranular cracking occurs much less often. Intergranular cracking is characterized by a path that follows the prior austenitic grain boundaries, while transgranular cracking occurs around the martensitic platelet boundaries. Many references contain explanations as to what factors may influence the mode of cracking. These include composition, microstructure, environment, annealing, aging effects, and geometry, each of which are discussed in the following pages.

C.8.2 Effect of Composition on SCC Fracture Path

When comparing the results of chemical analysis of both materials, it is evident that only the cobalt content was significantly different. As listed in one source, some hardening results from a short-range ordering reaction in the matrix involving cobalt, but it appears that the main contribution of cobalt is to lower the solubility of molybdenum in the martensite matrix and thus increase the amount of Ni_3Mo precipitate.[7] Cobalt is added to maraging steels to lower the Ms temperature and thereby produce a finer microstructure according to the ASM Specialty Handbook.[8] No difference in hardness or grain size was noted between the Ft. Lewis and the HAAF specimens. Other sources[9, 10] indicate that the primary strengthening effect of this alloy comes from the combination of cobalt and molybdenum. Most importantly, however, according to the ASM Specialty Handbook cobalt additions increase the time-to-failure for maraging steels in stagnant 3.5% NaCl.[8] This is illustrated graphically in Figure 21 of the ASM Specialty Handbook).[8] Although these data were generated for the 250 Grade (no such data was found for the 300 Grade), the specimens were proof-ring type (not bent-beam type), and the specimens were immersed in salt water (not within a salt fog environment), it does show the effect cobalt has on the time-to-failure of maraging steel. The differences shown graphically in Figure C-21 are for 8% nominal cobalt (top curve), 2% nominal cobalt (middle curve), and cobalt-free (bottom curve). The tests were conducted in stagnant 3.5% NaCl solution for 1000 hr using proof-ring speciments.[7] The specimens in the ARL study only differed by 0.43 weight-percent (9.77 minus 9.34 weight-percent). However, with the lack of any other contributory factor, it is believed that the difference in cobalt composition may have attributed to the extended duration times Ft. Lewis specimens, as compared to the HAAF specimens.

---

[7] ASM. *ASM Metals Handbook, Ninth Edition, Volume 1, Properties and Selection: Irons and Steels.* "Maraging Steels," p. 446, 1978.

[8] ASM. *ASM Specialty Handbook, Carbon and Alloy Steels.* "Corrosion Behavior," pp. 465–466, 1996.

[9] Vishnevsky, C. "Literature Survey on the Influence of Alloying Elements on the Fracture Toughness of High Alloy Steels." AMMRC CR 69-18/1, Interim Report, Contract DAAG 46-69-C-0060, Army Materials and Mechanics Research Center, Watertown, MA, pp. 31, 32, February 1970.

[10] Psioda, J. A., and J. R. Low, Jr. "The Effect of Microstructure and Strength on the Fracture Toughness of an 18 Ni, 300 Grade Maraging Steel." NASA Technical Report No. 7, Carnegie Mellon University, Department of Metallurgy and Materials Science, Pittsburgh, PA, p. 13, August 1975.
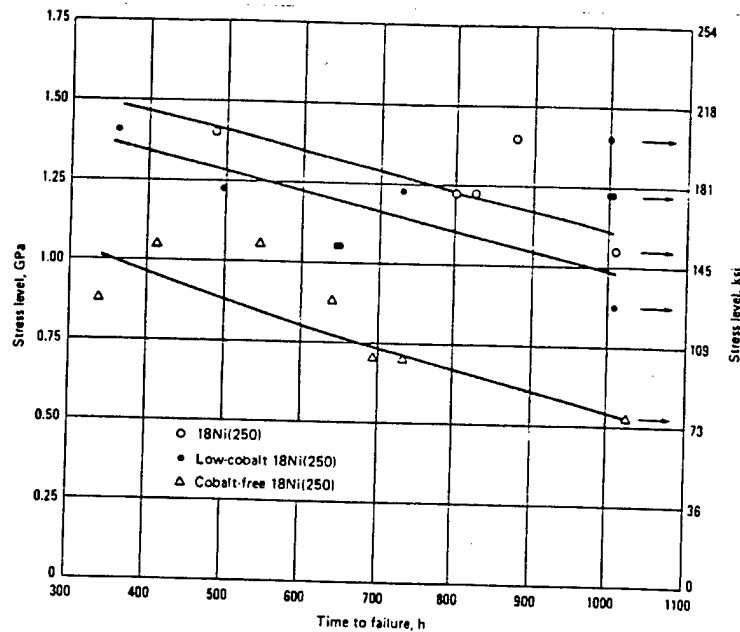
Figure C-21. Chart showing the effect of increased cobalt composition on
the time-to-failure of maraging 250 steel. Plot compares
8% cobalt, 2% cobalt, and cobalt-free maraging 250 steel.
Tests were conducted in stagnant 3.5% NaCl solution for
1000 hr using proof-ring specimens.

C.8.3 Effect of Microstructure on SCC Fracture Path

It has previously been shown that crack propagation rates within high-strength steels are generally faster at higher strength levels and are greatly dependent on microstructure.[11] Generally, maraging steel with a coarse grain size does not offer the time-to-failure resistance of finer grained maraging steel. The structures and grain size of specimens coated at each facility were similar; therefore, it was determined that the microstructure had no effect.

C.8.4 Effect of Environment on SCC Fracture Path

Because the pH, temperature, and the sodium chloride concentration for all testing were kept at specified levels within the salt fog chamber, it is highly unlikely that the environment had a role in the different fracture paths.

---

[11] Wanhill, R. J. H. "Microstructural Influences on Fatigue and Fracture Resistance in High Strength Structural Materials." *Engineering Fracture Mechanics*, vol. 10, p. 351, 1978.

C.8.5 Effect of Annealing on SCC Fracture Path

It has been shown that coarse grain size is detrimental to SCC resistance for 300 grade maraging steels according to Dautovich and Floreen.[6] Subsequent failure occurs along the prior austenitic grain boundaries, and results in shorter time-to-failure values. The landing support struts are required to be annealed at $1500° \pm 25$ °F. Higher annealing temperatures (in excess of 1500 °F) produce larger grains within the structure of maraging steels. Because the grain size of both the HAAF and Ft. Lewis specimens was similar, and within specification, it was determined that prior annealing temperatures had no effect on the fracture path.

C.8.6 Effect of Aging on SCC Fracture Path

Open literature contains the effect of aging treatments and times on the hardness of maraging steels.[10] The range of aging treatments listed in this reference is from 600° to 1000 °F. The required aging range for the shock strut mount is 900 °F $\pm$ 25 °F. In general, the high strength of maraging alloys is developed by aging,[12] and it has also been shown that crack rates in a 350 grade maraging steel could be varied over 2 orders of magnitude by changes in the aging temperature.[11] Therefore, different aging treatments could produce material with different hardness levels. However, the fact that the hardness measurements were similar for both the HAAF and Ft. Lewis specimens indicates that prior aging was not an issue.

C.8.7 Effect of Geometry on SCC Fracture Path

Crack path observations in this material are somewhat difficult to interpret because SCC attack generally produces intergranular fractures, while transgranular morphologies may occur as a result of geometry.[13] This does not explain the phenomenon noted by ARL because the geometry was similar for each specimen (bent-beam specimens 4 in $\times$ 0.75 in $\times$ 0.10 in).

---

[12] Battelle. *Aerospace Structural Metals Handbook.* "18 Ni Maraging (300)," Metals and Ceramics Information Center, Columbus Division, Columbus, OH, p. 1, 1987.

[13] Jeanfils, C., C. A. Pampillo, and H. W. Paxton. "The Effect of Reverted Austenite on the Stress Corrosion Cracking Resistance of Two Maraging Steels." Office of Naval Research Technical Report N00014-67-A-0314-0004, p. 3, November 1971.

C.9 Conclusions

Although the Ft. Lewis specimens outperformed the HAAF specimens with respect to time-to-failure within the salt fog chamber, the specimens were practically similar in every way. The specimens were sectioned from two different shock strut mounts, but in the same locations. The specimens were loaded into similar fixtures and loaded to similar levels. The hardness of both sets of specimens was similar, as was the brush cadmium thickness, the grain size, and the microstructure.

One difference was noted: the Ft. Lewis specimens contained more cobalt than the HAAF specimens. Increased cobalt has been shown to increase the time-to-failure of maraging steels with respect to SCC. It may be possible that the difference in cobalt composition was enough to prolong the time-to-failure of the Ft. Lewis SCC specimens in the salt fog environment.

Appendix D. Grain Size Comparison of Failed Strut Mount, Hunter Army Air Field (HAAF) Specimen and Ft. Lewis Specimen

D.1 Background

The grain size of failed Shock Strut Mount P/N 7-311113409, determined to be approximately double the required size (refer to section 2), was compared to the grain size of two scrap strut mounts. These strut mounts included one which had been sectioned into specimens that were cadmium brush plated at HAAF, Savannah, GA, and one that was sectioned for brush plating at Ft. Lewis, WA. The governing material specification, HMS 6-1081, *18% Nickel Maraging Steel - Bars and Forgings, 300,000 psi (2069 Mpa) Yield Strength* Grade, requires a grain size of no. 7 or finer with an occasional no. 5. It was determined that the grain size of the failed strut mount was between American Society for Testing and Materials (ASTM) nos. 2 and 3. Figure D-1 shows the grain size of the failed part, with a grain size reticle overlay at 100× magnification. Figure D-2 shows a scanning electron micrograph of the actual grain size observed within the intergranular fracture surface at 200× magnification.

Figure D-1. Grain size of the failed strut mount with reticle overlay (mag. 100×).
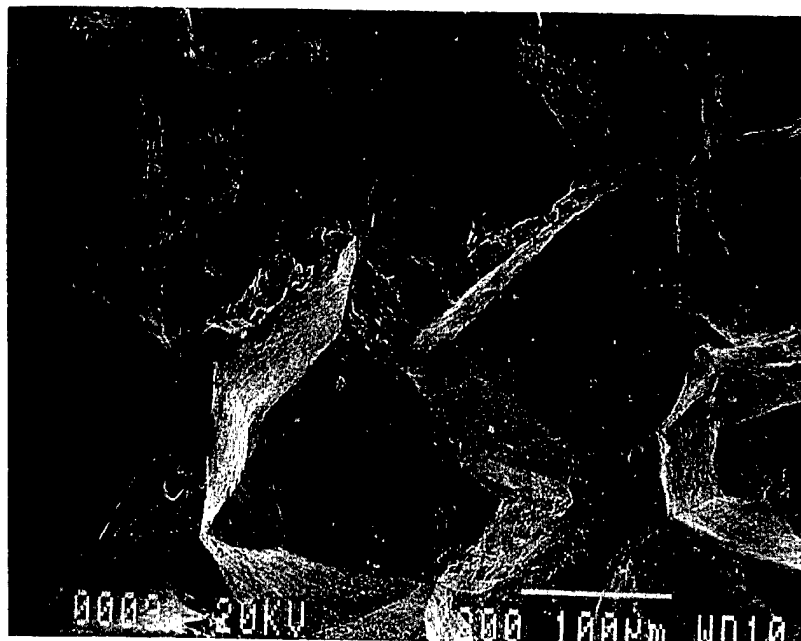
Figure D-2. Grains from the intergranular fracture surface of the failed strut mount (mag. 200×).

D.2 HAAF Specimen Grain Size

For comparative purposes, the grain sizes of the scrap strut mounts were documented in a similar manner. Specimens were sectioned from these struts, cadmium brush plated at the two facilities, and loaded into a three-point bend fixture in accordance with ASTM G39.[1] The test fixtures were subsequently placed into a salt fog chamber and tested in accordance with ASTM B117[2] until failure. A representative failed stress corrosion test specimen from both HAAF and Ft. Lewis was sectioned and metallographically prepared. Figure D-3 shows the grain size of the HAAF strut mount with the reticle overlay. These grains measured between nos. 6 and 7. Compare to the grains shown in Figure D-1. Figure D-4 shows the fracture surface of the HAAF specimen that had failed in the salt fog chamber. Compare these grains to those of the failed strut mount (Figure D-2).

D.3 Ft. Lewis Specimen Grain Size

Similarly, the Ft. Lewis specimen grain size was documented, as shown in Figure D-5 with the reticle overlay. The size of these grains were similar to those observed within the HAAF specimen. Also, the fracture surface of the stress corrosion cracking (SCC) specimen is shown in Figure D-6 at 200× magnification. Although the mode of failure was mixed mode (transgranular, occurring along the martensitic platelets with evidence secondary cracking), the cracking occurred at the austenitic grain boundaries, allowing for grain size comparison. Again, the grain size was similar to the HAAF specimen.

---

[1] American Society for Testing and Materials. "Standard Practice for Preparation and Use of Bent-Beam, Stress Corrosion Test Specimens." ASTM G39, West Conshohocken, PA, pp. 1–7, 1994.

[2] American Society for Testing and Materials. "Standard Practice for Operating Salt Spray (Fog) Apparatus." ASTM B117, West Conshohocken, PA, 1997.
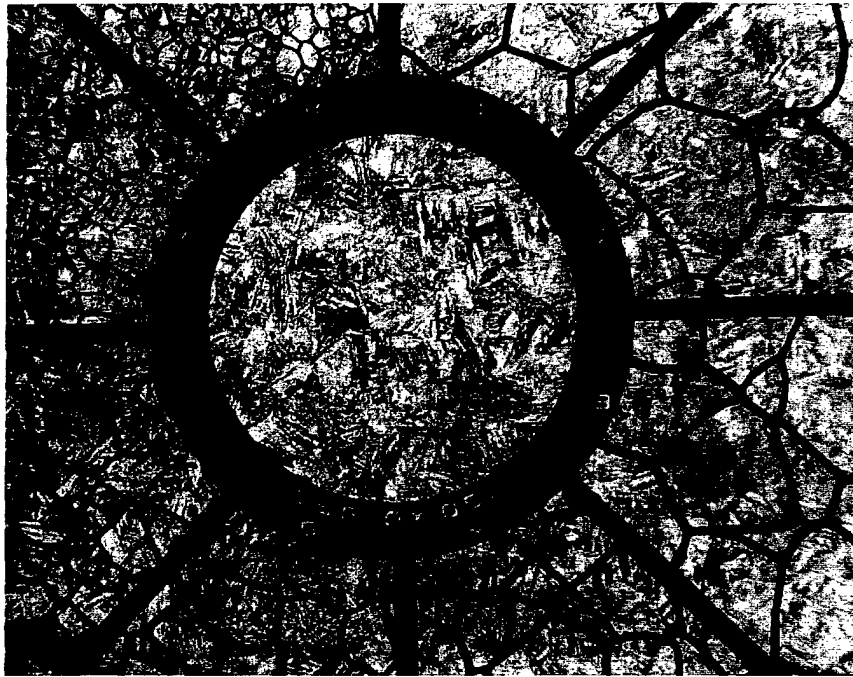
Figure D-3. Grain size of the HAAF specimen with reticle overlay.
Compare to Figure D-1 (mag. 100×).
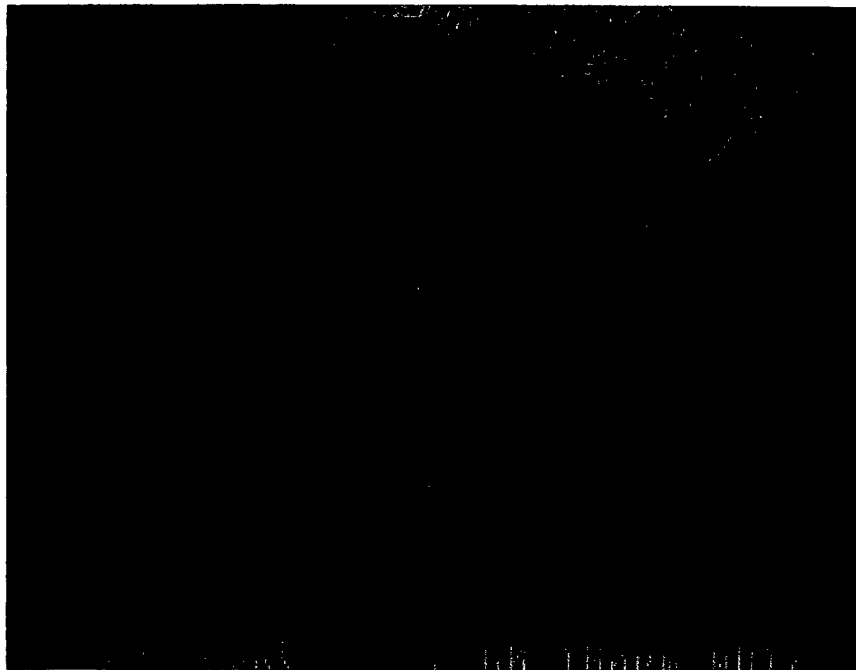
Figure D-4. Grains from the intergranular fracture surface of the HAAF SCC
specimen. Compare to Figure D-2 (mag. 200×).

Figure D-5. Grain size of the Ft. Lewis specimen with reticle overlay.
Compare to Figure D-1 (mag. 100×).
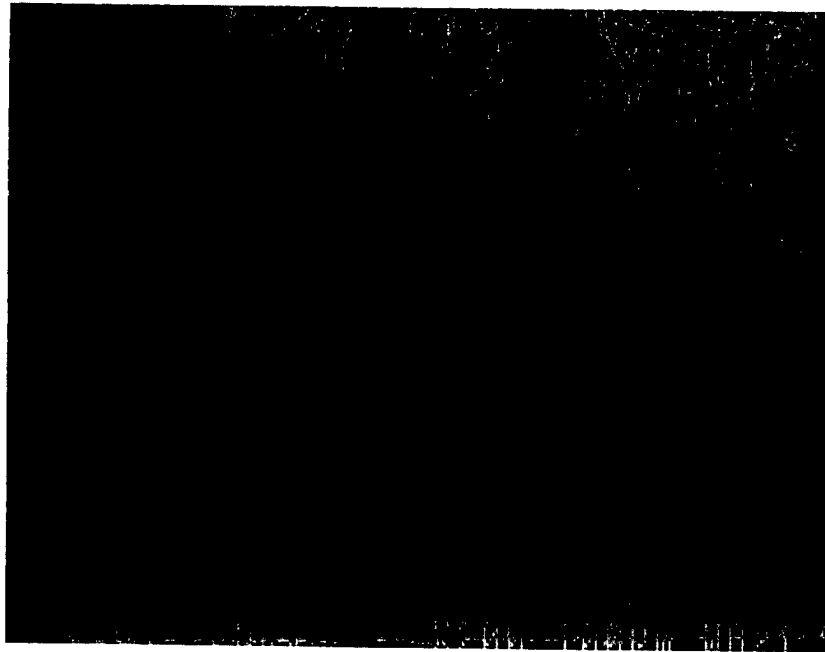
Figure D-6. Grains from the intergranular fracture surface of the Ft. Lewis SCC
specimen. Compare to Figure D-2 (mag. 200×).

D-4. Conclusion

This study was undertaken in order to compare the grain size previously noted within the
failed strut mount to that of two additional strut mounts. This comparison is further evidence
that the failed strut mount contained a grain size that was larger than specified.

Appendix E. U.S. Army Aviation and Missile Command (AMCOM) Deficiency Report

As a result of the failure analysis performed by the U.S. Army Research Laboratory, a Category I/Category II Deficiency Report was issued by AMCOM. This type of report is submitted when there is a critical failure, and in this case, it details a description of the problem, and the short- and long-term recommendations concerning the shock strut mount. The AMCOM deficiency report is included as an attachment in this appendix.

Category I/Category II Deficiency Report (CAT I/CAT II DR)	DATE JAN 2 2 1998
HQ, U.S. ARMY AVIATION AND MISSILE COMMAND (AMCOM) Bldg. 5681 Redstone Arsenal, AL. 35898-5000	OFFICE SYMBOL AMSAM-AR-E-I-P-A (702-3b)

TO:

Commander
D Company, 3/229TH Aviation Regiment
ATTN: Sean Faulk
Fort Bragg, NC 28307-5000

REPORT CONTROL NUMBER W8TR4970003		SUBJECT Category I Deficiency Report on R/H MLG Mount Failure
PREPRINTED CONTROL NO M18H90009	AIRCRAFT AH64A	

1. Reference Category 1 Deficiency Report W8TR4970003 AMCOM Control No. M18H90009.

2. The referenced Category 1 Deficiency Report indicates a failure of the Right Hand(R/H) Main Landing Gear Mount which secures the R/H Landing Gear Trailing Arm to the fuselage. The Mount failed during flight. The pilot landed on a support after the failure to prevent further damage. This is the first mount to fail during flight.

3. The cause of numerous failures of this item is stress corrosion initiating at the transition point between the base of the underside of the shaft and the mount base. This is a result of the cadmium plating flaking off or being worn off the shaft. The current inboard beveled washer if installed improperly will wear away the plating. It is uncertain as to how effective this surface will be protected with MIL-P-23377 primer when the plating is gone. Several OLR sites are being qualified to use brush cadmium plating to more adequately protect this area.

4. To prevent the mount from separating a bolt will be installed through the hollow shaft. This should prevent the aircraft from listing if the mount should fail. This is only a temporary solution. The kits to perform this installation are scheduled to be issued shortly. Contact Jim Mason at DSN 876-4242.

TYPED NAME AND TITLE BARRY J. BASKETT Director of Aviation Engineering	SIGNATURE

DRSTS-M Form 42
1 Aug 77

Replaces DRSAV-F Form 42, 1 May 77, which may be used.

2

5. The solution to this problem is to retrofit the entire fleet with redesigned Mounts made from stainless alloy which is much less susceptible to stress corrosion. They will not require plating to prevent them from failing as is the current design. In addition, a new inboard bevel washer has been designed to replace the existing one. The design of this item is such that the washer can not be inadvertently installed backwards.

6. Funding to retrofit this new mount to the entire fleet is currently an unresolved issue.

7. Until the new mounts are available or the safety bolt MWO has been applied, request that all personnel exercise extreme caution while working under or on the aircraft and be alerted to the possibility of this failure mode.

8. Steps will be taken to reduce the time between inspections to help mitigate the risk of mount failure. You will be informed immediately of these changes in inspection interval.

9. McDonnell Douglas Helicopter Systems will be tasked with this QDR response to initiate a field study to perform a crack propagation test on a cracked Main Landing Gear Mount. This test will provide badly needed data to access the amount of time involved to fail the Mount once a crack is initiated.

10. Send Failed Mount to:
COMMANDER, U.S. ARMY AVIATION AND MISSILE COMMAND (AMCOM),
ATTN: AMSAM-AR-E-I-P-A (Bumbicka), Bldg 5681,
Redstone Arsenal, AL 35898-5000

11. This DR is closed.

12. The Point of Contact for this action is Lee Bumbicka, AMSAM-AR-E-I-P-A, DSN 897-4925, Commercial 205-313-4925, E-Mail: bumbickal@avrdecr.redstone.army.mil.

CF:
Project Manager, Apache Attack Helicopter,
   ATTN: SFAE-AV-AAH-S
Defense Contract Management Command Boeing Phoenix-Mesa
   McDonnell Douglas Helicopter Systems, ATTN: DCMCDW-GPOMB,
   BLDG 510, Mail Station A277, 5000 East McDowell Rd., Mesa, AZ
   85215-9797
Commander, U.S. Army Aviation and Missile Command,
   ATTN: AMSAM-AR-Z-A-TS, AMSAM-MMC-US-A, AMSAM-MMC-LS-DC,
   AMSAM-MMC-RE-FD, AMSAM-MMCRE-LU

3

INTENTIONALLY LEFT BLANK.

Appendix F. Change of Manufacturer's Engineering Drawing

Because this part has had a history of failures, the manufacturer performed an engineering study and concluded that a change in the alloy used to make this component was necessary. Corrosion resistant precipitation hardenable PH 13-8Mo steel was chosen to be the replacement for the high-strength maraging steel. Another change, was that the part would now be required to be shot peened (which was not a requirement for the maraging steel component). The change to the manufacturer's engineering drawing is shown as an attachment in this appendix.

For Interpretation See A-130000000 REV M

================= PARTS LIST REVISION BLOCK =================

Rev	EO Number	Authority	Release Date	Design Org Code Code		Rev	EO Number	Authority	Release Date	Design Org Code Code
C	6456974	CP4193	97 JAN 28	DRUM 42IN		A	6454023	GS007H	96 96C 09	DRLO DRLO
B	6456759	CP4193	97 JAN 22			-	0451010	GS007H	96 FEB 20	DRLO

================= PARTS DESCRIPTION BLOCK =================

Find No.	Dwg Zone	Quantity Required					-2	-1	UM	FSCM	Part Number/ Natl Ident Nbr	Nomenclature	(Specification)	Notes
1							END	EA	8V613	7-311113709-1	MOUNT, FORGING - SHOCK STRUT, MLG		
							END	EA	8V613	7-311113709-2	MOUNT, FORGING-SHOCK STRUT,MLG,RH		
					90;	PS	LB	02731	MX50-1100+PBARN SXFSXSRS	CRES BAR,PH13-8,S.S THK 5.5 WD (Part Number continued)		

================= NOTES BLOCK =================

No.	Type	Line	NOTES: UNLESS OTHERWISE SPECIFIED.	Component Part Number	Dwg Zone	Canned Note Number
1	G	1	DIMENSIONING AND TOLERANCING PER ANSI Y14.5M 1982.			
2	G	1 2	THE UG MODEL IS CONSIDERED BASIC AND HAS NO TOLERANCE.			
3	G	1	EDGE AND CORNER RADII .31 +/- .125.			
4	G	1	FILLET AND INTERNAL CORNER RADII .03 +/- .125.			
5	G	1	DRAFT ANGLE = 5 DEGREES +/- 1 DEGREE.			
6	G	1 2 3 4 5 6 7	TOLERANCES: FLASH EXTENSION: .25 MAXIMUM DIE MISMATCH: .09 MAXIMUM STRAIGHTNESS: .12 MAXIMUM THICKNESS ON PARALLEL SURFACES: + .19 PER INCH - .03 PER INCH FORGING DIMENSIONS IN DIRECTION			

THIS IS A CONTROLLED SERIALIZED ITEM

Notes continued on next page.

PL7-311113709   Rev C   Sheet 1

================= NOTES BLOCK (continued) =================

No.	Type	Line	NOTES: UNLESS OTHERWISE SPECIFIED.	Component Part Number	Dwg Zone	Canned Note Number
6	G	5 6 7 8	ELONGATION 12.0% FOR LONGITUDE 12% FOR TRANSVERSE REDUCTION OF AREA 50% FOR LONGITUDE 65% FOR TRANSVERSE			
7	G	1	MACHINE FINISH RHR125 OR BETTER.			
8	G	1	THREADS PER HANDBOOK H28 AND MIL-STD-9.			
9	G	1	LAST SECTION OR VIEW USED: L			
10	G	1	DELETED			
11	*	1 2 3 4 5 6	SHOT PEEN AROUND INDICATED AREAS PER HP4-56 SHOT SIZE .011 TO .028 INTENSITY .008 TO .012 A, 200% COVERAGE UNIFORM FADE OUT AREA FOR SHOT PEEN 1 INCH MINIMUM BEYOND INDICATED AREA. AS AN OPTION ENTIRE PART MAY BE SHOT PEENED EXCEPT FOR THREADED AREA.			
12	*	1 2	IDENTIFY PER HP8-5, TYPE 1, CLASS 4. SERIALIZE PER HP8-8.			
13	*	1	OMIT PRIMER FROM THIS SURFACE.			
14	*	1 2 3	SEE TABLE ZONE 12H FOR HOLE LOCATIONS. TABULATED DIMENSIONS ARE BASIC. TOOL 7-311113709-1-1TC1 MAY BE USED AS AN ALTERNATE TO TABULATED DIMENSIONS.			
15	*	1	DIMENSION TO BE MET PRIOR TO SHOT PEEN.			
16	*	1	DRY FILM LUBE PER HP4-75, TYPE 1, THREADED AREA ONLY.			
17	*	1	TRIM RADIUS FEATHER EDGES TO .02/.06.			
SER		1	DENOTES A SERIALIZED COMPONENT PART.			

Note Type: G = General Note * = Flag Note S = Service Note

End of Parts List   PL7-311113709   Rev C   Sheet 2 of 2

REPORT DOCUMENTATION PAGE		Form Approved OMB No. 0704-0188

Public reporting burden for this collection of information is estimated to average 1 hour per response, including the time for reviewing instructions, searching existing data sources, gathering and maintaining the data needed, and completing and reviewing the collection of information. Send comments regarding this burden estimate or any other aspect of this collection of information, including suggestions for reducing this burden, to Washington Headquarters Services, Directorate for Information Operations and Reports, 1215 Jefferson Davis Highway, Suite 1204, Arlington, VA 22202-4302, and to the Office of Management and Budget, Paperwork Reduction Project(0704-0188), Washington, DC 20503.

1. AGENCY USE ONLY (Leave blank)	2. REPORT DATE November 2002	3. REPORT TYPE AND DATES COVERED Final, 1997–January 2002	
4. TITLE AND SUBTITLE Failure Analysis, Cadmium Brush Plate Qualification and Salt Fog Testing of the AH-64 Shock Strut Mount, P/N 7-311113409			5. FUNDING NUMBERS AH80
6. AUTHOR(S) Marc Pepi			
7. PERFORMING ORGANIZATION NAME(S) AND ADDRESS(ES) U.S. Army Research Laboratory ATTN: AMSRL-WM-MD Aberdeen Proving Ground, MD 21005-5069			8. PERFORMING ORGANIZATION REPORT NUMBER ARL-TR-2870
9. SPONSORING/MONITORING AGENCY NAMES(S) AND ADDRESS(ES) Dr. Kirit Bhansali U.S. Army Aviation and Missile Command Redstone Arsenal, Huntsville, AL 35898			10.SPONSORING/MONITORING AGENCY REPORT NUMBER

11. SUPPLEMENTARY NOTES

12a. DISTRIBUTION/AVAILABILITY STATEMENT Approved for public release; distribution is unlimited.	12b. DISTRIBUTION CODE

13. ABSTRACT(Maximum 200 words)

A failure analysis was performed on a shock strut mount from an AH-64 Apache attack helicopter. It was concluded that the failure was attributed to stress corrosion cracking and/or corrosion fatigue and had initiated at a region where the protective cadmium plating was worn away in service. Based upon this conclusion, it was necessary to qualify two facilities (Hunter Army Air Field, Savannah, GA and Ft. Lewis, Dupont, WA) for the cadmium brush plating rework of these components found to have worn coatings during routine inspections. The U.S. Army Research Laboratory was involved in the qualification process for both facilities, and the results of each quality audit are included. Finally, the results of salt fog testing of cadmium brush plated specimens, plated at the respective facilities, are also included, as well as a comparison of the grain size of the material in the failed component vs. the material from the struts plated at each facility.

14. SUBJECT TERMS failure analysis, maraging steel, stress corrosion cracking			15. NUMBER OF PAGES 77
			16. PRICE CODE
17. SECURITY CLASSIFICATION OF REPORT UNCLASSIFIED	18. SECURITY CLASSIFICATION OF THIS PAGE UNCLASSIFIED	19. SECURITY CLASSIFICATION OF ABSTRACT UNCLASSIFIED	20. LIMITATION OF ABSTRACT UL

NSN 7540-01-280-5500

Standard Form 298 (Rev. 2-89)
Prescribed by ANSI Std. 239-18   298-102

INTENTIONALLY LEFT BLANK.